Bull. Min. Res. Exp. (2018) 157: 121-152

Bulletin of the Mineral Research and Exploration

http://bulletin.mta.gov.tr

Mineral chemistry, whole-rock geochemistry and petrology of Eocene I-type shoshonitic plutons in the Gölköy area (Ordu, NE Turkey)

İrfan TEMİZEL[a*], Emel ABDİOĞLU YAZAR[b], Mehmet ARSLAN[c], Abdullah KAYGUSUZ[d] and Zafer ASLAN[e]

[a]*Karadeniz Technical University, Department of Geological Engineering, 61080, Trabzon, Turkey. orcid.org/0000-0002-6293-8649*
[b]*Karadeniz Technical University, Department of Geological Engineering, 61080, Trabzon, Turkey. orcid.org/0000-0001-5196-8060*
[c]*Karadeniz Technical University, Department of Geological Engineering, 61080, Trabzon, Turkey. orcid.org/0000-0003-0816-4168*
[d]*Gümüşhane University, Department of Geological Engineering, 29000, Gümüşhane, Turkey. orcid.org/0000-0002-6277-6969*
[e]*Balıkesir University, Department of Geological Engineering, 10145, Balıkesir, Turkey. orcid.org/0000-0002-3418-4368*

Research Article

Keywords:
Mineral chemistry, thermobarometer, geochemistry, I-type, monzonite, Eocene, Gölköy, Turkey

Received Date: 21.06.2017
Accepted Date: 27.12.2017

ABSTRACT

The Eocene intermediate to felsic plutons are widespread in varying sizes and compositions throughout the Eastern Pontides Orogenic Belt in NE Turkey. Of these, two monzonitic bodies (namely the Eriko Tepe and Göl Tepe Plutons) in the Gölköy (Ordu) area, extend nearly in the orientation of NW-SE and E-W and were emplaced into the Upper Cretaceous and/or Eocene volcanic and sedimentary rocks. Petrographically, the studied monzonitic plutons are compositionally fine to medium grained monzonite, monzodiorite and subordinate quartz-monzonite. They consist of plagioclase (An_{35-67}), K-feldspar (Or_{61-96}), quartz, clinopyroxene ($Wo_{28-49}En_{35-51}Fs_{10-25}$), biotite (Mg#: 0.53-0.73) ± hornblende (Mg#: 0.65-0.82), Fe-Ti oxide with monzonitic, poikilitic, perthitic, rare antirapakivi and graphic textures. Mineral thermobarometer estimations imply that the plutons were crystallized in P-T conditions of mid to shallow crustal levels. Petrochemically, these monzonitic plutons show post-collisional, I-type, metaluminous (A/CNK=0.76-0.93) and shoshonitic features. The whole-rock major oxide and trace element variations suggest that fractionational crystallization played a significant role in the evolution of these monzonitic plutons. The primitive mantle-normalized trace element patterns of the studied plutons are similar to each other with enrichment in large ion lithophile elements, Th, Ce and negative Nb and Ti anomalies. Moreover, the chondrite-normalized rare earth element plots of the plutons show moderately enriched concave-shaped patterns (La_N/Lu_N=9.3-12.6) with negative Eu anomalies (Eu_N/Eu^*=0.69-0.84), all of which imply plagioclase and clinopyroxene ± hornblende fractionations during their evolution. The geochemical data suggest that the monzonitic plutons have evolved from parental magmas derived from the melts of enriched lithospheric mantle, in a post-collisional setting.

1. Introduction

The plutons observed in the Eastern Pontides Orogenic Belt (EPOB) have a wide age interval from Paleozoic to Tertiary, and they are formed by mafic and felsic rocks mainly ranging from gabbro to granite. These plutons have intruded in three time periods mainly during the Permo-Carboniferous, Cretaceous and Eocene. Of these, the Permo-Carboniferous granitoids (Yılmaz, 1972; Çoğulu, 1975; Topuz et al., 2010; Dokuz, 2011; Kaygusuz et al., 2012, 2016) were emplaced into the metamorphic rocks. The Cretaceous granitoids have a contact relation with volcanic and/or volcanoclastic rocks related to subduction (Yılmaz and Boztuğ, 1996; Karslı et al., 2010*a*; Kaygusuz et al., 2008, 2009, 2010, 2011, 2012; Kaygusuz and Aydınçakır, 2009, 2011; Kaygusuz and Şen, 2011; Karslı et al., 2012*a*; Kaygusuz et al., 2013, 2014). On the other hand, the fewer Eocene and post Eocene granitoids have cut all the series in narrow areas (Yılmaz and Boztuğ, 1996; Aslan et al., 1999; Topuz, 2002; Arslan and Aslan, 2006; Karslı et al., 2007;

* *Corresponding author: İrfan TEMİZEL, itemizel@ktu.edu.tr*
http://dx.doi.org/10.19111/bulletinofmre.371623

2011, 2012*b*; Kaygusuz and Öztürk, 2015).

In the eastern part of the EPOB (especially in Gümüşhane and Bayburt regions) there have been many studies of the geochemistry, petrogenesis and the geochronology of some of the Eocene plutons (eg. Arslan and Aslan, 2006; Karslı et al., 2007; 2011, 2012*b*; Kaygusuz and Öztürk, 2015). There are limited radiometric ages of the Eocene plutonic rocks in the region, and the age of many plutons were determined by the contact and stratigraphic relationships. However, Eocene plutons located in the Gölköy (Ordu) locality in the western part of the region and its surrounding have not been subject to any detailed petrographical, geochemical or petrological investigation. We present here the first mineral chemistry and whole-rock geochemistry of the Eocene monzonitic plutons outcropping on two different areas (Eriko Tepe and Göl Tepe) in the southeastern of Gölköy. From this we are able to establish the petrochemical and magma-tectonic characteristics and the genesis and evolution of the magmas (differentiation ± contamination).

2. Regional Geology

Turkey is a significant part of the Alpine-Himalayan orogenic belt and consists of remnants of the Paleotethys and Neotethys oceanic basins among the tectonic units (Pontides, Anatolides, Taurides and Margin folds) extending nearly in the E-W directions (Figure 1a) (Şengör and Yılmaz, 1981). Geological events related to the Paleotethys have prevailed in the Sakarya Zone and the Central Pontides in N-NW Turkey and completed its evolution by being unconformably overlain by Liassic sediments (Şengör and Yılmaz, 1981). In addition the geological events related to the Neotethys have affected the whole of Anatolia from Triassic to Miocene (Şengör and Yılmaz, 1981). The Late Cretaceous and Tertiary granitoid magmatism is one of the most significant orogenic events that have occurred during the closure of the Neotethys oceanic basins (Figure 1b).

The crustal basement of the Eastern Pontides (Ketin, 1966) is formed by Late Carboniferous granitoids, Late Carboniferous-Early Permian shallow marine-continental and the continental metasedimentary rocks (Yılmaz, 1972; Çoğulu, 1975; Okay and Leven, 1996; Topuz et al., 2007, 2010, 2011; Dokuz, 2011; Kaygusuz et al., 2012, 2016). The metamorphic rocks forming the basement have been cut by the Paleozoic granitoid rocks in pre-Liassic times (Çoğulu, 1975). The granitoid rocks mega plutonic masses and are observed in the Gümüşhane area and between the Köse area (Çoğulu, 1975; Topuz

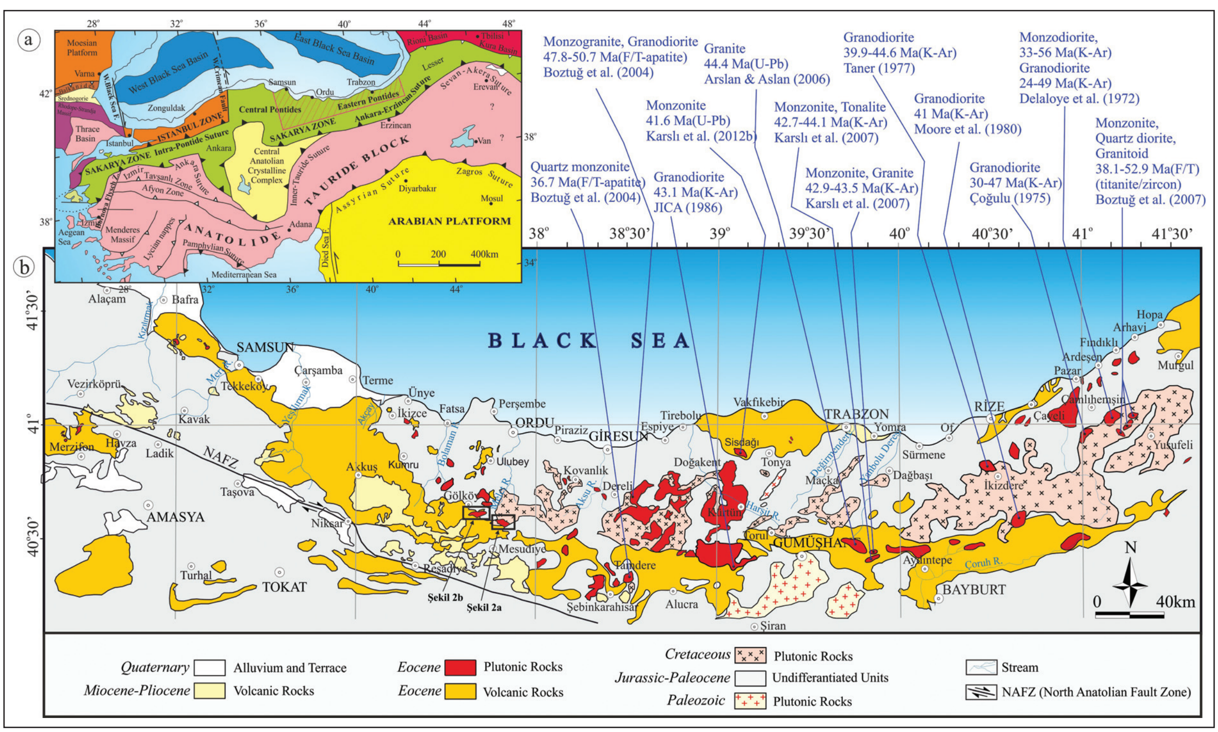

Figure 1- a) Tectonic map of Turkey (modified from Okay and Tüysüz, 1999), b) the distribution of plutonic rocks in the Eastern Pontides (modified from Güven, 1993; MTA, 2002; Arslan et al., 2013*a*; Temizel et al., 2016; Yücel et al., 2017) and the radiometric ages obtained from Eocene plutons.

et al., 2010; Dokuz, 2011), in the south of Tonya and Maçka (Soğuksu) area and the Özdil area (Kaygusuz et al., 2012, 2016). The Paleozoic rocks also form small outcrops around Artvin. The Early-Middle Jurassic pyroclastites, and clastic and sedimentary rocks intercalated with carbonates unconformably overlie the basement rocks in the Eastern Pontides and are interpreted as the volcano-sedimentary deposit related to the rift (Ağar, 1977; Robinson et al., 1995; Arslan et al., 1997; Kandemir, 2004; Dokuz and Tanyolu, 2006; Şen, 2007; Kandemir and Yılmaz, 2009). This unit is mainly represented by volcanic rocks in the northern part, and sedimentary deposits intercalating with tuff and tuffites in the south. During closure of the Paleotethys, and with the collision that occurred by the addition of the Sakarya zone in the north and Laurasia, the synchronous granitoids are Late Jurassic (Yılmaz et al., 1997; Dokuz et al., 2010) which through to the Early Cretaceous period was a period of stability in the whole orogenic belt and the carbonate deposition in the whole Eastern Pontides are dominant in this period (Pelin, 1977).

The Eastern Pontide magmatic arc developed in the Late Cretaceous along the southern boundary of the Sakarya Zone due to the northern subduction of the Neotethys (Okay and Şahintürk, 1997; Yılmaz et al., 1997; Topuz et al., 2007; Altherr et al., 2008; Dilek and Sandvol, 2009; Dilek et al., 2010; Ustaömer and Robertson, 2010; Rolland et al., 2012; Ustaömer et al., 2013; Topuz et al., 2013; Okay et al., 2013). There are different ideas about the direction and termination of the subduction of the Eastern Pontide magmatic arc, and the time of collision of the Tauride-Anatolide Platform and the Eurasian plate. These are; (1) the development of the Pontide arc as a result of the northern subduction from Paleozoic to Eocene (Ustaömer and Robertson, 1995; Okay and Şahintürk, 1997; Yılmaz et al., 1997), (2) the occurrence of the Paleotethys in the north of Pontides, and the presence of the southern subduction polarity starting from the end of the Paleozoic until the end of the Eocene (Dewey et al., 1973; Bektaş et al., 1984, 1999; Chorowicz et al., 1998; Eyüboğlu et al., 2011*a*), and 3) the presence of a two directional subduction polarity as being towards the south until Dogger and towards the north starting from the Late Cretaceous until the end of the Eocene for the Pontide arc (Şengör and Yılmaz, 1981). The Eastern Pontide magmatic arc system consists of a Late Cretaceous volcano-sedimentary deposit thicker than 2 km and the high-K, calc-alkaline, I-type granitoids (Yılmaz and Boztuğ, 1996; Okay and Şahintürk, 1997; Yılmaz et al., 1997; Boztuğ et al., 2003, 2004, 2006; Boztuğ and Harvalan, 2008; İlbeyli, 2008; Kaygusuz et al., 2008, 2009, 2010, 2011, 2012; Kaygusuz and Aydınçakır, 2011; Kaygusuz and Şen, 2011).

The collision of the Eastern Pontides magmatic arc and the Anatolide-Tauride continental block occurred in the Late Paleocene-Early Eocene (~55 Ma) and required a widespread shortening, crustal uplift and thickening, and flysch deposition in NE Turkey (Okay and Şahintürk, 1997; Dilek, 2006). The Eocene units in the Eastern Pontides generally overlie the Upper Cretaceous and Paleocene units with the basal conglomerate and are overlain by a series of andesite-basalt, pyroclastites and flysch deposits (Arslan and Aliyazıcıoğlu, 2001; Arslan et al., 2013*a*). The formation of the early Eocene adakitic rocks in the Eastern Pontides (54-48 Ma) (Topuz et al., 2005; Karslı et al., 2010*b*, 2011; Eyüboğlu et al., 2011*a, b, c*; Topuz et al., 2011; Eyüboğlu et al., 2013*a, b*; Karslı et al., 2013), corresponds to the last stage of the arc to continent collision, and they are associated with syn- and post-collisional origins. As for the Middle Eocene, the post collisional calc-alkaline volcanic rocks and high-K, calc-alkaline, shoshonitic granitoid plutons developed (Yılmaz and Boztuğ, 1996; Arslan et al., 1997; Şen et al., 1998; Aliyazıcıoğlu, 1999; Arslan and Aliyazıcıoğlu, 2001; Arslan et al., 2002; Boztuğ et al., 2004; Topuz et al., 2005; Arslan and Aslan, 2006; Karslı et al., 2007, Boztuğ and Harvalan, 2008; Temizel and Arslan, 2008, 2009; Aslan, 2010; Eyüboğlu et al., 2012; Karslı et al., 2012*b*; Temizel et al., 2012*a, b*; Yücel et al., 2012; Arslan et al., 2013*a, b*; Temizel, 2014; Yücel, 2013; Aslan et al., 2014; Temizel et al., 2014; Temizel et al., 2016; Yücel et al., 2017). The clastic rocks are widespread in the region in the post-Eocene (Okay and Şahintürk, 1997) and are generally accompanied by Neogene alkaline volcanic rocks (Aydın et al., 2008, 2009; Arslan et al., 2013*b*; Yücel, 2013, Yücel et al., 2012, 2014, 2017). The Quaternary deposits are represented by travertine and alluvial deposits.

3. Material and Methods

The field studies were carried out in two different areas where the Eocene Eriko Tepe and Göl Tepe plutonic bodies are located (Figures 2a, b).

Thin sections for the rocks of Eriko Tepe and Göl Tepe plutons were prepared in the thin section laboratory of the Geological Engineering Department

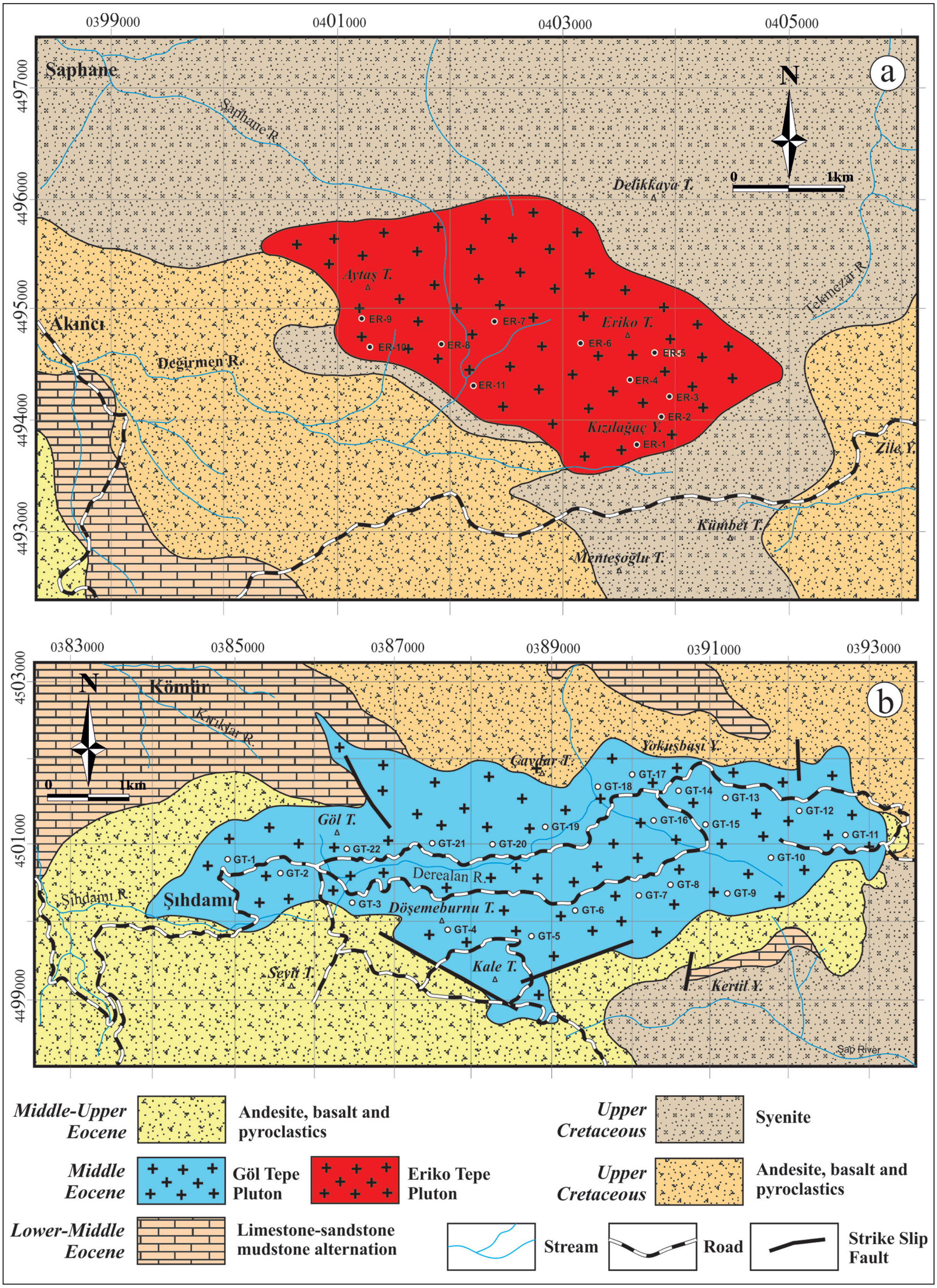

Figure 2- Geological maps showing the studied plutons and surrounding rocks of: a) the Eriko Tepe, and, b) the Göl Tepe plutons (modified from Güven, 1993; MTA, 2002, 2011).

at the Karadeniz Technical University and used to determine mineralogical compositions and textural-petrographical characteristics using a polarized microscope. The Swift point counter was used for the modal analyses and the counting was generally made within a 0.4 mm interval, but sometimes a 0.2 mm interval was also selected depending on the grain size. Approximately 400-500 points were counted in each thin section.

Mineral chemistry was determined using the CAMECA-SX-100 WDS electron microprobe in the Geoscience Marines (IFREMER) Electron Microprobe Laboratory (Universite de Bretagne Occidentale, Brest, France). The operating conditions were 15 kV and 20 nA, and a 10 µm beam diameter, and the count timing was 10s for Si, Al, Ti, Fe, Mn, Mg, Ca, Na and K. A 1 µm beam was used for pyroxene, hornbende and Fe-Ti oxide analyses. For feldspar and mica the very light defocused beam (10 µm) was used to prevent alkali loss. The natural mineral standards used were forsterite, diopside, orthoclase, albite, anorthite, biotite, apatite, wollastonite and magnetite. The analytical error is less than 1% for major elements and less than 200 ppm for trace elements.

The petrography guided the selection of fresh rock samples collected from the plutons and these were crushed by the steel jaw crusher in the Sample preparation and milling laboratory in the Geological Engineering Department at the Karadeniz Technical University. They were then pulverized in to an approximately 200 mesh size in a steel ring mill. Whole-rock analyses of rock powders from the plutons were undertaken at ACME Analytical Laboratories Ltd. (Vancouver, Canada). The major and trace element analyses were carried out by the Inductively Coupled Plasma Atomic Emission Spectrometer (ICP-AES) after fusing 0.2 gr powdered rock sample in 1.5 gr $LiBO_2$ then dissolving in 100 ml 5% HNO_3. The Rare Earth Element (REE) contents were analyzed by ICP-AES after dissolving 0.25 gr powdered rock sample in four different acids. The Loss of Ignition (LOI) was calculated from the weight difference after samples were ignited under temperature of 1000°C. The total iron content was expressed in terms of Fe_2O_3. The major elements were estimated in weight %, and the trace and REE were estimated in terms of ppm. The deviation limits in the analyses are 0.001-0.04% for major elements, 0.1-1 ppm for trace elements and 0.01-0.1 ppm for REE.

4. Geology and Petrography

4.1. Eriko Tepe Pluton

The Eriko Tepe Pluton covers nearly 7 km^2 in area and outcrops in the Eriko Tepe, Aytaş Tepe, Kızılağaç Valley and its surrounds in the south of Topçam town (Mesudiye, Ordu) (Figure 2a). The pluton was emplaced into Late Cretaceous andesite, basalt, pyroclastites, and syenites. Field observations and stratigraphical relationships of units indicate that the age of the pluton is Middle Eocene (Güven, 1993; MTA, 2002, 2011). The longitudinal axis of the Eriko Tepe Pluton extends in the northwest-southeast direction (Figure 2a) and outcrops in the form of heads on the field (Figure 3a, b). They are medium to fine grained and generally grey to dark grey due to high amounts of ferromagnesian minerals. Minor silicification and epidotization were observed where the pluton was in contact with the country rocks.

The plutonic rocks generally exhibit monzonitic, poikilitic, perthitic and rarely antirapakivi textures with plagioclase, orthoclase and quartz, with lesser ferromagnesian minerals which are clinopyroxene, biotite and hornblende (Figure 3c-f). However in some samples the hornblende is abundant with lesser biotite and pyroxene. Apatite, zircon and sphene are the opaque and accessory minerals and are less frequent than other minerals.

Plagioclases (25-30 modal %) are fine and coarse euhedral-subhedral grains that generally show albite polysynthetic twinning, but rarely Carlsbad twinning (Figure 3c) or oscillatory zoning. They are andesine (An_{44-46}) in composition based on extinction angle determinations on sections perpendicular to the (010) plane of plagioclases that show twinning based on the Albite law. The Carlsbad twinning was observed in some of the anhedral orthoclases (30-35 modal %) with variable sizes. The perthitic intergrowths, characterized by albite exsolution lamellae, were also detected in orthoclase. The coarse orthoclase crystals have occasional plagioclase, clinopyroxene and biotite inclusions in a poikilitic texture (Figure 3e-f) and surround plagioclase as monzonitic textures in some sections. Quartz grains (5-11 modal %) are anhedral and fine grained. They were emplaced generally into the residual empty spaces as it is the latest crystallized production of the magma (Figure 3c-f). Clinopyroxenes are subhedral and contain abundant opaque mineral inclusions (Figure 3c-f); their extinction angles are nearly 40° and so defined

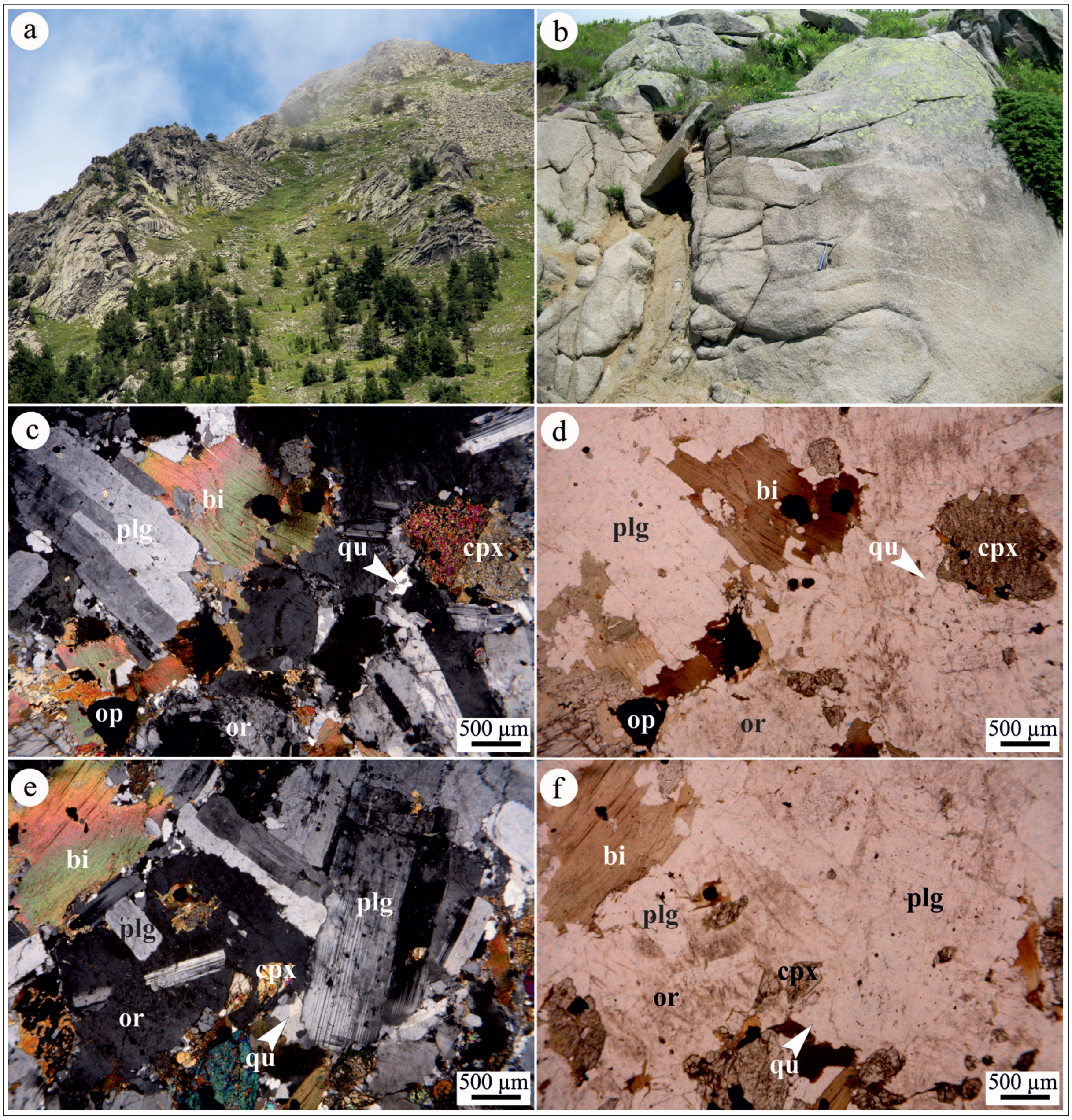

Figure 3- The field view (a and b) of the Eriko Tepe plutons and micro photos of the monzonite which exhibit the granular texture; (c and d) the plagioclase with Carlsbad twinning, bending in biotites that consists of opaque mineral inclusions and corrosions at the circumferences of clinopyroxenes; (e and f) the monzonitic texture formed by the enclosure of plagioclase by orthoclase, and the enclosure of clinopyroxene and biotite by the orthoclase in poiklitic texture, the albite-carlsbad complex twinning in plagioclases (Sample No: ER-2; C.N. and P.N.) (Explanations: C.N.: cross nicol; P.N., parallel nicol; cpx; clinopyroxene; bi: biotite; pl: plagioclase; or: orthoclase; op: opaque).

as augite. In some of their crystals the h' (100) twining was detected (Figure 3c). Biotite (8-10 modal %) are generally subhedral-euhedral and the parallel cleavage to (001) plane is distinctive. The brown pleochroism is distinctive and it is dark brown in z and y directions and yellowish in the x direction. They generally exhibit kink-banding due to deformation (Figure 3c-f). Hornblende (4-6 modal %) is few but where present is euhedral-subhedral and fine grained. and with green to pale green pleochroism. The extinction angle between c^z was measured as 20°. The mafic minerals in the rock are clustered: clinopyroxene and hornblende is surrounded, respectively, by biotite and opaque minerals and the formation of biotites around the clinopyroxene identifies disequilibrium crystallization. Opaque minerals (5-8 modal %) are subhedral-anhedral fine crystals and are as inclusions in, and surrounding, the mafic minerals (Figure 3c-d). The majority of samples collected from the Eriko Tepe Pluton have not been affected from the alteration. Sericitization of plagioclases is rare and chloritization of ferromagnesian minerals is observed in some samples.

Modal analysis of 12 plutonic samples (Table 1), and the Quartz-Alkaline Feldspar-Plagioclase (QAP) diagram (Streickeisen, 1976) identified that the pluton is monzonite and quartz monzonite in composition (Figure 4).

Table 1- The general petrographical characteristics and modal compositions of the rocks from the Eriko Tepe and the Göl Tepe Plutons.

Name of the Pluton	**ERİKO TEPE PLUTON (ER) (n=12)**			**GÖL TEPE PLUTON (GT) (n=13)**		
Rock Type	Monzonite, Quartz monzonite			Monzonite, Quartz monzonite		
Texture	Monzonitic, poikilitic, perthitic, antirapakivi			Monzonitic, poikilitic, graphic, perthitic		
Grain Size	Medium-fine			Medium-fine		
Modal Min. (%)	**Mean**	**Min.**	**Max.**	**Mean**	**Min.**	**Max.**
Plagioclase	25.48	18.25	29.78	34.21	26.99	44.15
Quartz	5.19	1.25	10.36	3.87	0.58	9.44
Orthoclase	31.27	19.42	34.89	27.26	19.65	35.00
Hornblende	4.61	1.95	6.00	4.84	2.56	7.42
Biotite	8.04	7.06	9.99	6.76	1.12	9.36
Pyroxene	10.47	3.65	15.03	9.56	5.12	16.87
Access. Min.	2.23	1.83	2.63	1.39	0.56	2.25
Opaque Min.	5.44	2.85	8.46	6.22	4.11	8.92
Secondary Min.	3.07	2.21	4.68	2.66	0.20	6.10

n= the number of rocks on which the modal analysis were performed.

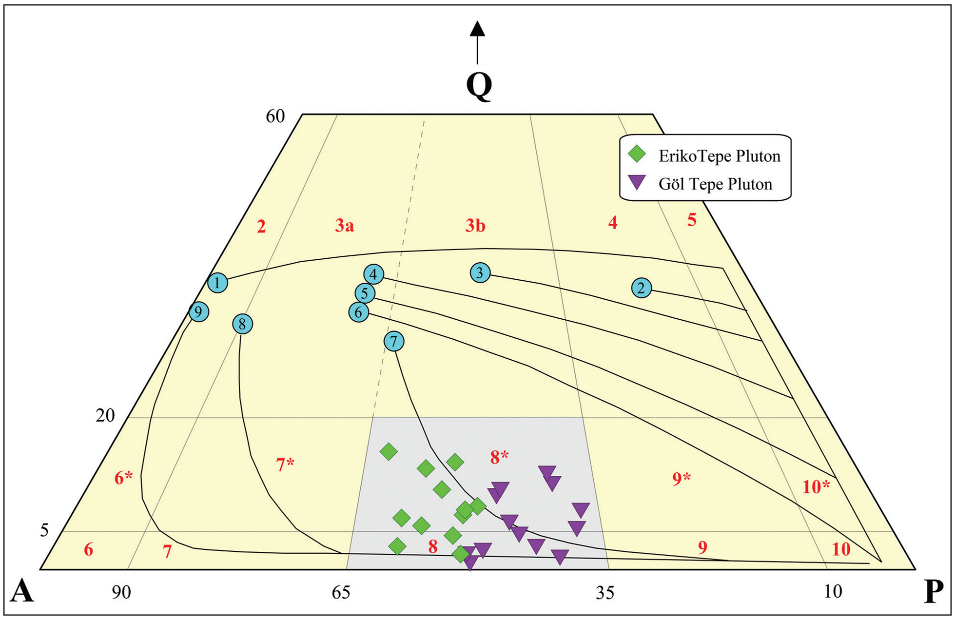

Figure 4- The Q-A-P plot of the rock samples from the Eriko Tepe and Göl Tepe Plutons. The curves show the directions of plutonic type series, which are: 1) tholeiitic series, 2) calc-alkaline trondhjemite series, 3-6) variable calc-alkaline granodioritic series, 7) monzonitic series, 8-9) variable alkaline series (Lameyre and Bonin; 1991). The fields; (2) alkaline feldspar granite, (3a) syenogranite, (3b) monzogranite, (4) granodiorite, (5) tonalite, (6*) quartz alkaline feldspar granite, (7*) quartz syenite, (8*) quartz monzonite, (9*) quartz monzodiorite/quartz monzogabbro, (10*) quartz diorite/quartz gabbro/quartz anorthosite, (6) alkaline feldspar granite, (7) syenite, (8) monzonite, (9) monzodiorie/ monzogabbro, (10) diorite/gabbro/anorthosite (Streckeisen, 1976).

4.2. Göl Tepe Pluton

The Göl Tepe Pluton outcrops in the Göl Tepe, Şıhdamı, Döşemeburnu Tepe, Kale Tepe, Çavdar Tepe, Yokuşbaşı Valley and surrounding areas in the south of the Gölköy (Ordu) town (Figure 2b). It is emplaced into a sedimentary series formed by the intercalation of Late Cretaceous andesite, basalt, pyroclastites and syenites, with Early-Middle Eocene limestone, sandstone, and mudstone (Figure 2b). The pluton is Middle Miocene based on stratigraphic relationships (Güven, 1993; MTA, 2002, 2011) and extends in the east-west direction (Figure 2b) and outcrops in the form of heads on the field with very hard, jointed and fractured structures (Figure 5a, b). Some outcrops are

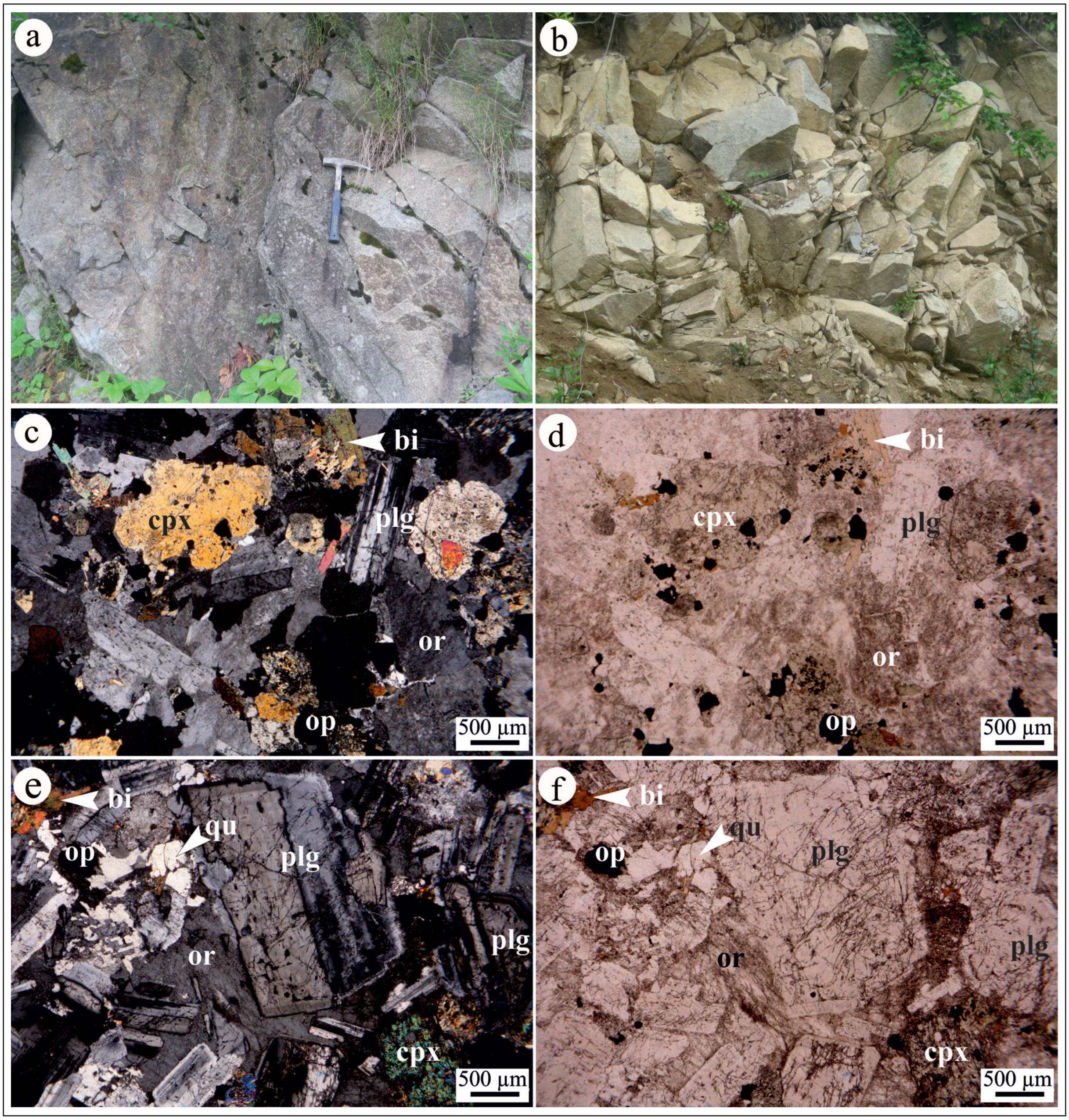

Figure 5- Monzonites from the Göl Tepe Pluton exhibit much fragmented and fractured structure (a and b), and the micro photos of monzonites that show granular textures; (c and d) the plagioclase minerals that show albite, albite-carlsbad complex twinning, clinopyroxene and biotite that have opaque mineral inclusions (Sample No: GT-3; C.N. and P.N.), (e and f) the plagioclase with oscillatory zoning in which the irregular growths are seen, the clinopyroxene mineral, which consists of much opaque minerals and plagioclase inclusions, and the monzonitic texture formed by the inclusion of plagioclase by orthoclase (Sample No: GT-4; C.N. and P.N.) (cpx; clinopyroxene; bi: biotite; plg: plagioclase; qu: quartz; or: orthoclase; op: opaque).

dark grey, depending on mineral content, and fine to medium grained. Contacts between the pluton and the country rocks are restricted by the NW-SE, NE-SW and N-S directional normal faults (Figure 2b) and crushed zones are seen occasionally in areas where the faults are observed. Rare examples of silicification and epidotization are noted.

Monzonitic, poikilitic, graphic and occasionally perthitic textures are observed and the felsic minerals present are plagioclase and quartz, whereas the dark colored minerals are clinopyroxene, hornblende and biotite and accompanying opaque minerals (Figure 5 c-f). Pyroxene, hornblende and biotite minerals are clustered and are accompanied by opaque minerals (Figure 5c, d). Accessory minerals are zircon and apatite.

Plagioclases (33-44 modal %) are euhedral-subhedral, fragmented and broken with albite twinning and oscillatory zoning, and both in some grains. Their composition is andesine (An_{40-44}) according to the examination of the perpendicular sections of crystals (010) with albite twinning. Only plagioclases with the zoned structures have irregular growth (Figure 5e, f). In some samples, there are minor opaque and apatite inclusions. Orthoclase (27-35 modal %) is anhedral and common. Some exhibit Carlsbad twinning, the others show perthitic texture (Figure 5c, f). Poikilitic grains tend to contain plagioclase, pyroxene, hornblende and opaque minerals, forming monzonitic textures surrounding plagioclase in some samples. Quartz (4-9 modal %) is anhedral, fine grained and with undulose extinction (Figure 5e, f). Clinopyroxene is subhedral-anhedral, fragmented and is coarse and fine grained. The extinction angles between c^z are nearly 40°, and so is augite, and with rare h' (100) twinning but with common plagioclase, biotite and opaque inclusions (Figure 5c, f). Biotite (6-9 modal %) is subhedral-anhedral (Figure 5c, f) and have a typical yellowish brown to brown pleochroism, and with one directional well defined cleavage. Hornblende (5-7 modal %) is subhedral and fine grained, with green to pale green pleochroism and two directional hornblende cleavages (110) detected in some sections. Opaque minerals have a irregular geometrical shape and are located around ferromagnesian minerals, or, in the form of inclusions. Alteration is in the form of kaolinization of orthoclase, chloritization of ferromagnesian minerals and sericitization of plagioclases.

Modal analysis of 13 plutonic samples (Table 1), and the QAP diagram (Streickeisen, 1976) identified that the pluton is monzonite and quartz monzonite in composition (Figure 4).

5. Mineral Chemistry

Plagioclases in the Eriko Tepe Plutonic rocks are andesine and labradorite and their compositions vary between $An_{35-49}Ab_{48-64}Or_{0-5}$ and $An_{50-52}Ab_{47-48}Or_{1-2}$, respectively. K-feldspars in these rocks are orthoclase and their compositions vary between $An_{0-7}Ab_{6-31}Or_{64-94}$ (Figure 6a, Supplementary Table 1). Plagioclase in the rocks of the Göl Tepe Pluton is andesine and labradorite and their compositions vary between $An_{37-49}Ab_{47-59}Or_{1-4}$ and $An_{51-67}Ab_{32-46}Or_{1-4}$, respectively. The K-feldspars in these rocks are orthoclase and their compositions vary between $An_{0-4}Ab_{4-38}Or_{61-96}$ (Figure 6a, Supplementary Table 1).

Hornblendes in the Eriko Tepe Plutonic rocks are magnesiohornblende based on the classification of Leake et al. (1997) and the $Mg/(Mg+Fe^{2+})$ ratios vary between 0.65-0.82 (Figure 6b, Supplementary Table 2).

Clinopyroxenes in the Eriko Tepe Plutonic rocks are diopside, diopsitic augite and augite based on the classification of Morimoto et al. (1988) and their compositions and $Mg/(Mg+Fe^{2+})$ ratio vary between $Wo_{28-48}En_{37-51}Fs_{13-22}$ and 0.70-0.76, respectively (Figure 6c, Supplementary Table 3). Clinopyroxenes in the Göl Tepe Plutonic rocks are also diopside, diopsitic augite and augite (based on the classification of Morimoto et al. 1988) and their compositions and $Mg/(Mg+Fe^{2+})$ ratios vary between $Wo_{38-49}En_{35-46}Fs_{10-25}$ and 0.58-0.81, respectively (Figure 6c, Supplementary Table 3).

Biotites in the Eriko Tepe Plutonic rocks plot on the biotite area in the Fe/(Fe+Mg) vs Al^{IV} (apfu) diagram and their $Mg/(Mg+Fe^{2+})$ ratios vary between 0.53-0.60 (Figure 6d, Supplementary Table 4). In the Göl Tepe Plutonic rocks, based on the same plot, are classified as Mg enriched biotite and their $Mg/(Mg+Fe^{2+})$ ratios vary between 0.66-0.73 (Figure 6d, Supplementary Table 4).

Fe-Ti oxides in the Eriko Tepe Pluton are magnetite and titano-magnetite, and occasionally contain ilmenite lamellae (Supplementary Table 5) and in the Göl Tepe Pluton are also magnetite and titano-magnetite (Supplementary Table 5).

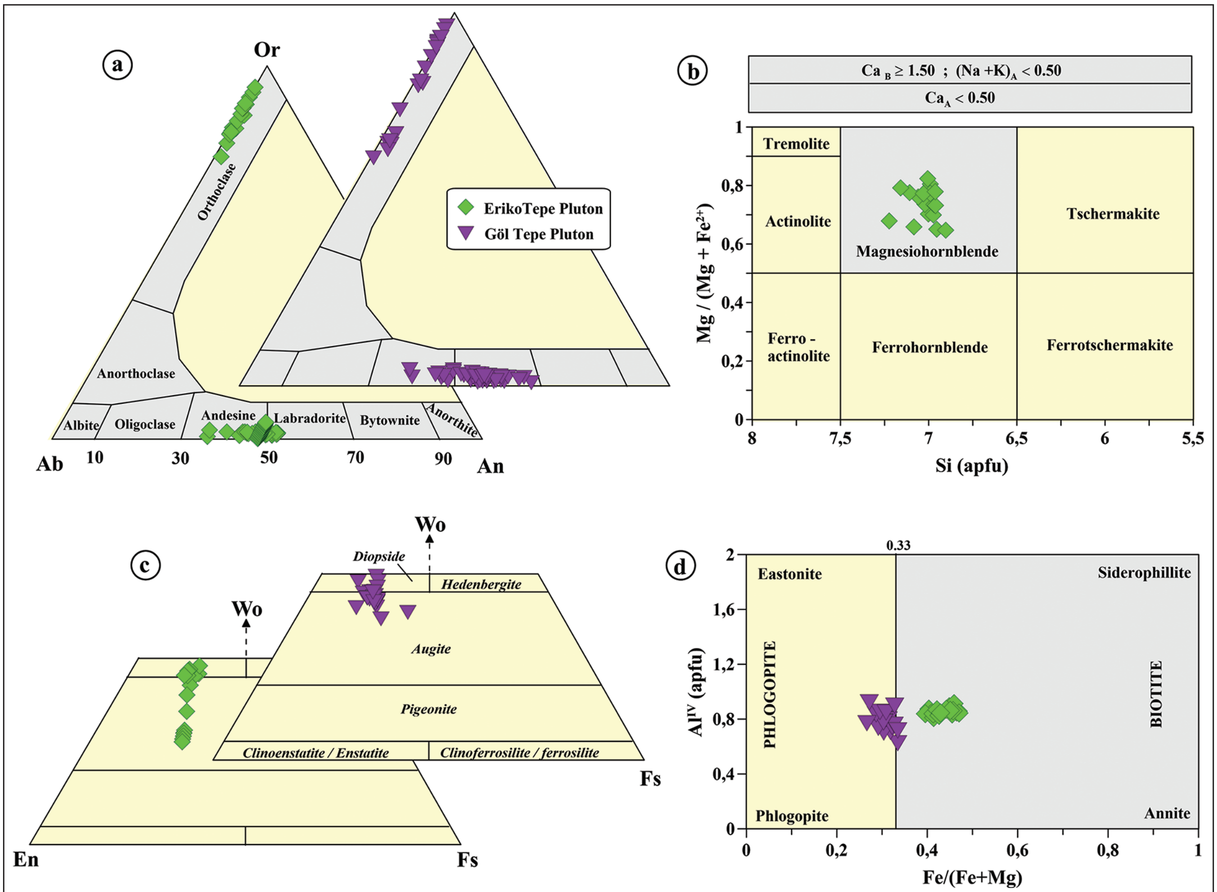

Figure 6- a) An-Ab-Or ternary plot of feldspars (Deer et al., 1992), b) Si (apfu) vs Mg/(Mg+Fe^{2+}) (Leake et al., 1997) classification diagram of hornblendes, c) Wo-En-Fs ternary plot of pyroxenes (Morimoto et al., 1988) and d) Mg–Li (apfu) vs Fe(t)+Mn+Ti-Al^{VI} (apfu) (Tischendorf et al., 1997) plot of biotites for the Eriko Tepe and the Göl Tepe plutonic rocks.

6. Whole-Rock Geochemistry

The major, trace and REE analyses for the Eriko Tepe and Göl Tepe Plutonic rocks are presented in Table 2. The geochemical characteristics of the major oxide and trace elements were compared in order to establish their magma-tectonic environments.

Plotting samples from both plutons on a TAS plot (Total alkali-silica, Middlemost 1994), the Eriko Tepe Pluton is in the monzonite field, and the Göl Tepe Pluton is in the monzodiorite, monzonite and quartz monzonite fields (Figure 7a). They are both alkaline (Figure 7a) again on this diagram based on the alkaline-subalkaline discrimination of Miyashiro (1978). The Eriko Tepe and the Göl Tepe plutonic rocks are shoshonitic on the SiO_2 (%) vs K_2O (%) diagram (Figure 7b) of Le Maitre et al. (2002), high-K and shoshonitic (Figure 7c) in character on the Co (ppm) vs Th (ppm) diagram of Hastie et al. (2007). On the (AI=Na+K/Al) vs (A/CNK) diagram of Maniar and Piccoli (1989) (Figure 7d), all samples are in the I-type field and metaluminous in character.

The rocks of the Eriko Tepe and the Göl Tepe Plutons present similar trends in major and trace element variation diagrams. With the increase in SiO_2 content, the K_2O, Na_2O, Rb, Zr, Nb, Ba, Hf, Th and Ta contents also increase, but on the contrary; TiO_2, Fe_2O_3*, MgO, MnO, CaO, P_2O_5, Sr and Y contents decrease (Figures 8 and 9). In addition; there is an increase then a decrease in the content of Al_2O_3 with the increase in SiO_2 content. The primitive mantle normalized trace element plots of the rocks from the studied monzonitic plutons exhibite similar distributions showing an enrichment in the large ion lithophile elements (LILE; Sr, K_2O, Rb and Ba), and in Th and Ce concentrations, but a depletion in some high field strength elements (HFSE; Y and TiO_2), and in Nb and Ta contents (Figure 10a). The chondrite normalized REE distributions for the rocks of the plutons are defined by a concave shaped

Table 2- The major (%), trace (ppm) and rare earth element (ppm) analyses for the rocks of the Eriko Tepe and the Göl Tepe Plutons.

	Eriko Tepe Pluton								Göl Tepe Pluton						
Sample no:	**ER-1**	**ER-2**	**ER-3**	**ER-4**	**ER-5**	**ER-6**	**ER-7**	**ER-8**	**GT-1**	**GT-2**	**GT-3**	**GT-4**	**GT-6**	**GT-7**	**GT-8**
SiO_2	58.08	56.56	56.22	58.16	57.63	55.98	59.06	59.06	53.80	55.98	55.58	55.01	53.34	64.16	55.18
TiO_2	0.77	0.83	0.82	0.69	0.78	0.79	0.63	0.68	0.80	0.68	0.67	0.72	0.72	0.40	0.71
Al_2O_3	16.44	16.28	16.92	17.12	16.59	16.40	15.79	16.98	17.09	17.40	17.74	17.18	16.83	16.14	17.02
Fe_2O_3(t)	7.21	8.06	7.81	6.27	7.33	7.70	6.33	6.21	8.68	7.20	7.29	7.71	8.27	4.26	7.80
MnO	0.13	0.15	0.14	0.20	0.13	0.14	0.10	0.14	0.16	0.14	0.14	0.14	0.16	0.10	0.13
MgO	3.11	3.59	3.47	2.58	3.17	3.49	3.11	2.52	3.38	3.07	3.01	3.22	3.62	1.51	3.44
CaO	5.56	6.20	6.25	4.69	5.61	6.37	5.43	4.43	6.53	6.18	6.38	6.78	6.75	3.57	6.18
Na_2O	3.11	2.97	3.09	3.53	3.14	2.97	3.03	3.53	3.17	3.40	3.20	3.54	3.19	3.13	2.97
K_2O	4.64	4.28	4.23	4.89	4.68	4.20	4.44	4.81	4.19	4.49	4.56	4.05	3.87	5.21	4.12
P_2O_5	0.34	0.35	0.35	0.32	0.32	0.35	0.26	0.29	0.35	0.34	0.34	0.35	0.35	0.17	0.34
LOI	0.3	0.4	0.4	1.2	0.3	1.3	1.5	1.1	1.5	0.8	0.8	1.0	2.5	1.1	1.8
Total	99.69	99.67	99.70	99.65	99.68	99.69	99.68	99.75	99.65	99.68	99.71	99.70	99.60	99.75	99.69
Zr	175.9	152.4	146.6	187.1	212.0	201.6	151.7	183.9	173.0	174.9	162.5	162.8	152.2	194.8	169.1
Y	20.8	22.7	20.1	23.8	20.8	20.4	19.0	22.9	21.6	20.9	20.9	19.9	21.1	16.6	20.8
Sr	704.1	784.3	765.3	668.3	706.0	752.7	635.5	651.8	896.0	787.9	775.9	756.8	1069.2	561.5	772.6
Rb	167.8	151.8	137.7	136.0	161.1	148.1	156.0	142.8	153.1	164.3	149.6	157.2	137.4	199.0	137.2
Th	18.8	12.4	12.0	11.5	15.3	13.3	15.7	13.9	10.5	13.3	10.8	12.5	11.3	18.6	12.0
Ta	0.8	0.7	0.7	0.7	0.7	0.7	0.7	0.8	0.4	0.6	0.7	0.7	0.7	1.0	0.5
Sc	16	18	17	14	16	18	16	14	17	15	15	16	18	7	17
V	193	232	212	166	198	228	174	157	223	180	176	201	222	90	203
Pb	4.2	2.0	1.5	11.9	3.9	1.7	5.8	4.5	5.3	5.9	12.4	9.9	9.7	10.0	3.2
Ni	10.7	13.5	13.4	7.2	11.7	12.9	12.1	7.6	10.7	10.0	9.7	11.8	14.4	5.6	15.0
Co	18.6	21.9	19.9	12.9	19.3	20.6	15.5	14.1	21.0	18.4	16.8	19.5	21.2	9.2	19.1
Cr	40	50	40	30	50	50	60	30	50	50	50	50	60	40	70
Cs	5.0	4.5	3.6	3.5	4.8	4.7	3.4	3.1	2.8	2.5	2.8	4.0	4.1	4.3	1.8
Ba	562	678	589	794	562	575	569	716	565	609	522	480	520	603	505
Nb	12.2	11.8	10.8	10.2	12.0	10.6	10.4	11.3	8.7	10.5	9.5	9.5	7.9	10.3	9.3
Hf	4.7	4.0	4.0	5.1	5.5	5.0	4.5	4.6	3.9	4.5	4.0	3.8	3.6	5.1	4.3
La	34.5	33.5	31.6	39.5	32.1	33.9	31.9	36.9	33.9	34.8	34.8	32.3	30.9	35.1	32.6
Ce	62.5	61.5	57.3	69.5	62.1	63.6	57.4	66.5	59.6	62.8	61.8	60.2	56.7	57.4	58.2
Pr	7.37	7.01	6.60	7.94	6.88	7.19	6.33	7.40	6.86	7.12	6.99	6.71	6.32	6.08	6.66
Nd	28.8	28.3	25.1	31.7	27.1	26.9	23.9	27.0	27.7	27.1	26.9	26.0	25.0	22.0	25.5
Sm	5.42	5.43	4.63	5.89	5.03	5.44	4.59	5.36	5.16	5.15	5.23	4.94	4.53	3.87	5.05
Eu	1.25	1.28	1.28	1.41	1.17	1.16	1.03	1.32	1.28	1.32	1.19	1.18	1.24	0.85	1.21
Gd	4.82	5.16	4.73	5.40	4.78	4.80	4.26	5.09	5.23	5.01	4.41	4.52	4.72	3.40	4.80
Tb	0.70	0.70	0.65	0.76	0.68	0.69	0.63	0.77	0.68	0.64	0.64	0.61	0.64	0.49	0.66
Dy	3.81	3.94	3.56	4.38	3.73	4.28	3.40	3.98	3.70	3.74	3.54	3.53	3.78	3.11	3.51
Ho	0.78	0.79	0.68	0.89	0.74	0.77	0.70	0.77	0.81	0.71	0.72	0.74	0.72	0.58	0.76
Er	2.14	2.29	2.15	2.41	2.19	2.05	1.91	2.28	2.07	2.16	2.07	2.13	1.91	1.72	2.08
Tm	0.36	0.35	0.30	0.36	0.30	0.32	0.30	0.37	0.31	0.34	0.32	0.32	0.29	0.27	0.32
Yb	2.25	2.29	2.11	2.44	2.20	2.14	2.00	2.42	2.25	2.10	2.00	2.07	2.17	1.97	2.17
Lu	0.35	0.35	0.33	0.40	0.36	0.33	0.31	0.39	0.35	0.36	0.35	0.30	0.33	0.29	0.34
Eu_N/Eu^*	0.75	0.74	0.84	0.76	0.73	0.69	0.71	0.77	0.75	0.79	0.76	0.76	0.82	0.72	0.75
La_N/Lu_N	10.23	9.94	9.94	10.25	9.26	10.66	10.68	9.82	10.06	10.04	10.32	11.18	9.72	12.57	9.95
La_N/Yb_N	10.36	9.89	10.12	10.94	9.86	10.70	10.78	10.30	10.18	11.20	11.76	10.54	9.62	12.04	10.15
Mg#	30.14	30.82	30.76	29.15	30.19	31.19	32.94	28.87	28.03	29.89	29.22	29.46	30.45	26.17	30.60

Fe_2O_3(t), total iron in terms of Fe_2O_3, LOI (Loss of Ignition): Total volatile content, Mg# =100 x MgO /[MgO + Fe_2O_3(t)].

pattern characterized with the presence of Eu anomaly (Figure 10b). The La_N/Lu_N ratios of the Eriko Tepe and Göl Tepe Plutons vary between 9.26-10.68 and 9.72-10.12.57, respectively and their La_N/Yb_N ratios vary between 9.86-10.94 and 9.62-12.04, respectively. On the other hand, the Eu_N/Eu^* ratios for the Eriko Tepe and the Göl Tepe plutons are in between 0.69-0.84 and 0.72-0.82, respectively (Figure 10b). The weak negative Eu anomaly of the plutonic rocks in the REE distributions indicates that the plagioclase

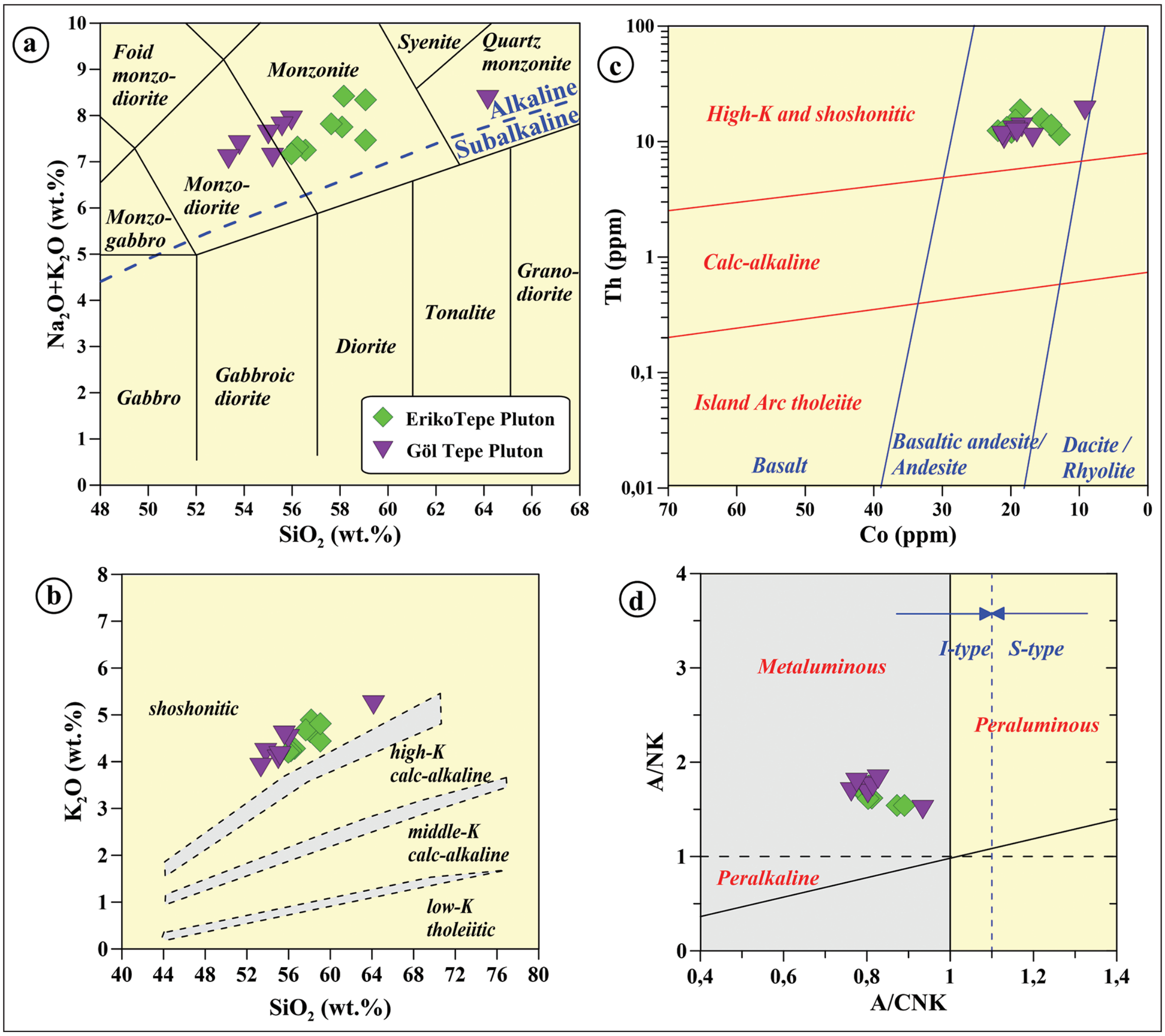

Figure 7- a) The classification diagram of Na_2O+K_2O (wt%) vs SiO_2 (wt%) (TAS) (Middlemost, 1994) (alkaline-sub alkaline line is based on Miyashiro (1978)), b) SiO_2 (wt%) vs K_2O (wt%) (Le Maitre et al., 2002), c) Th (ppm) vs Co (ppm) (Hastie et al., 2007), d) agpaitic index (AI=Na+K/Al) vs molar $Al_2O_3/(CaO+Na_2O+K_2O)$ (A/CNK) (Maniar and Piccoli, 1989) for the rocks of the Eriko Tepe and the Göl Tepe Plutons.

differentiation was not very effective in the evolution of these magmas (Figure 10b).

7. Discussion

The mineral chemistry and whole-rock analyses were used for the thermobarometry to reveal the P-T conditions. The data are also used to determine the source regions of the parental magmas, the role of magmatic processes in their evolution, and the magma-tectonic environments.

7.1. Crystallization Conditions of the Plutons

Temperature estimates are based on the two feldspar (plagioclase-alkaline feldspar) geothermometer (Putirka, 2003, 2005 and 2008), and they vary between 625-797 °C (mean= 726 ± 56ºC) for the Eriko Tepe Pluton and 623-770ºC (mean= 684 ± 47ºC) for the Göl Tepe Pluton (Table 3).

Temperatures based on the clinopyroxene thermobarometer (Putirka et al., 1996, 2003; Putirka, 1999, 2005, 2008), vary between 1039-1197ºC (mean= 1158 ± 49ºC) for the Eriko Tepe Pluton and 1018-1194ºC (mean= 1119 ± 47ºC) for the Göl Tepe Pluton (Table 4). The pressure values, on the other hand, vary between 5.3-8.4 kbar (mean= 7.5 ± 1.1 kbar) and 5.6-7.2 kbar (mean= 6.6 ± 0.6 kbar) for the Eriko Tepe Pluton and 3.2-6.6 kbar (mean= 4.8 ± 1.4 kbar) and 3.8-6.7 kbar (mean= 4.8 ± 1.3 kbar) for the Göl Tepe Pluton (Table 4).

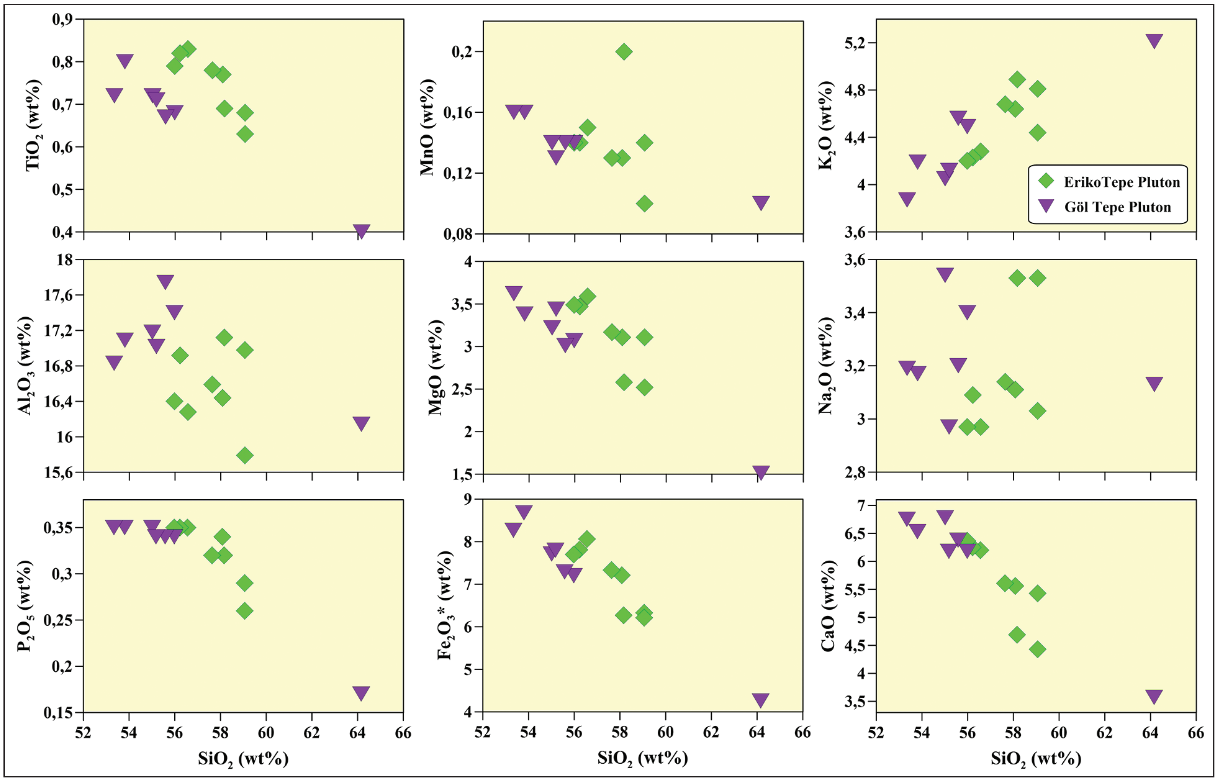

Figure 8- SiO_2 (wt%) vs major oxides (wt%) for the rocks of the Eriko Tepe and the Göl Tepe Plutons.

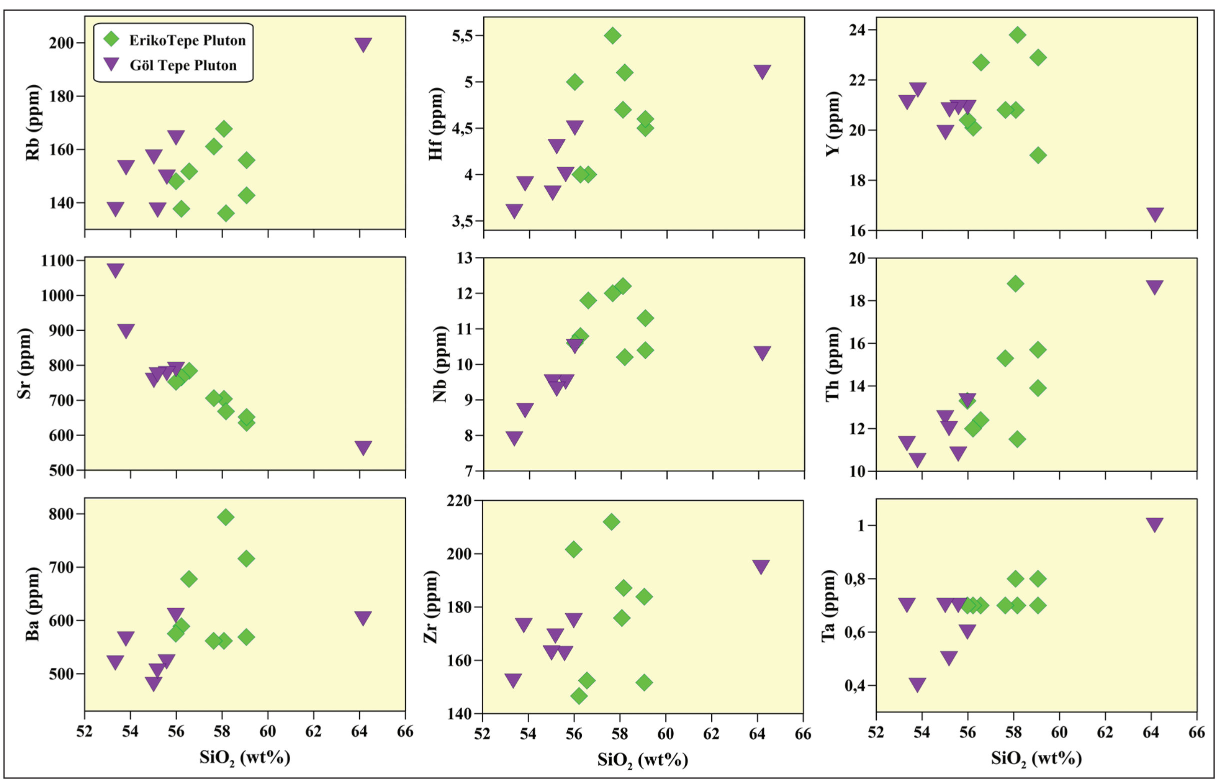

Figure 9- SiO_2 (wt%) vs trace elements (ppm) for the rocks of the Eriko Tepe and the Göl Tepe Plutons.

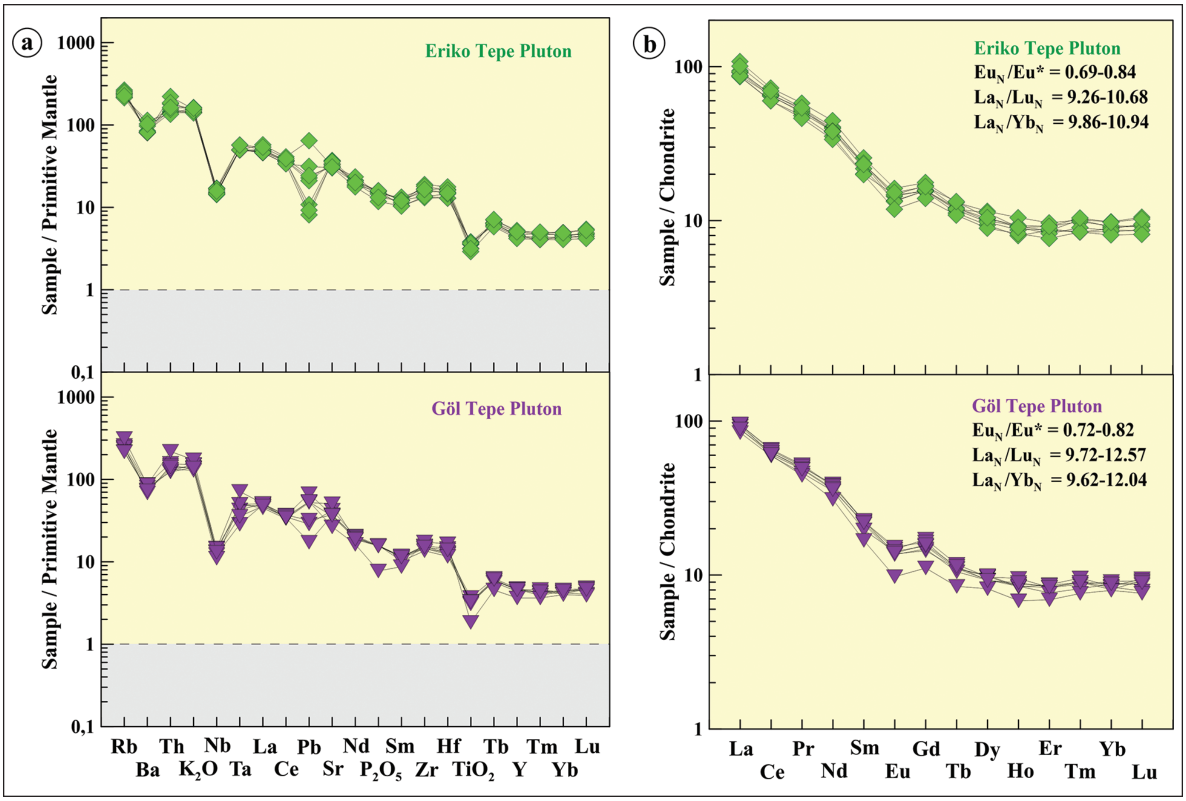

Figure 10- a) The primitive mantle normalized trace element distributions (Sun and McDonough, 1989) and b) the chondrite normalized rare earth element distributions (Taylor and McLennan, 1985) for the rocks of the Eriko Tepe and the Göl Tepe Plutons.

Table 3- The temperatures (T,ºC) estimated based on Putirka (2008) by using two feldspar compositions (plagioclase and alkaline feldspar) for the Eriko Tepe and the Göl Tepe Plutons.

Two feldspar (Plagioclase- alkaline feldspar) thermometer				
Equation 27b (thermometer)		**Mean T (°C)**	**Max. T (°C)**	**Min. T (°C)**
Eriko Tepe Pluton	(n=43)	726 ± 56	797	625
Göl Tepe Pluton	(n=24)	684 ± 47	770	623

Table 4- The temperatures (T,ºC) and pressures (P, kbar) estimated based on Putirka (2008) by using clinopyroxene and clinopyroxene-liquid compositions (plagioclase and alkaline feldspar) for the Eriko Tepe and the Göl Tepe Plutons.

Clinopyroxene Thermobarometer					
Equation 32a (barometer, non-aqueous)		**Max. P (kbar)**	**Min. P (kbar)**	**Mean P (kbar)**	**Mean Depth* (km)**
Eriko Tepe Pluton	(n=6)	8.4	5.3	7.5 ± 1.1	27.8
Göl Tepe Pluton	(n=4)	6.6	3.2	4.8 ± 1.4	17.8
Equation 32b (barometer, aqueous)					
Eriko Tepe Pluton	(n=6)	7.2	5.6	6.6 ± 0.6	24.4
Göl Tepe Pluton	(n=4)	6.7	3.8	4.8 ± 1.3	17.8
Equation 32d (thermometer, non-aqueous)		**Max. T (°C)**	**Min. T (°C)**	**Mean T (°C)**	
Eriko Tepe Pluton	(n=11)	1197	1039	1158 ± 49	
Göl Tepe Pluton	(n=13)	1194	1018	1119 ± 47	

* Depth was taken as 3.7 km for 1 kbar for the continental crust (Tulloch and Callis, 2000).

The pressure estimates based on the Al^T content of hornblende vary between 1.2-1.9 kbar (mean= 1.5 kbar ± 0.3 kbar) according to Hammarstrom and Zen (1986); 0.9-1.4 kbar (mean= 1.1 kbar ± 0.3 kbar) according to Hollister et al. (1987); 1.0-1.7 kbar (mean= 1.3 kbar ± 0.4 kbar) according to Johnson and Rutherford (1989) and 1.8-2.5 kbar (mean= 2.1 kbar ± 0.3 kbar) according to Schmidt (1992) (Table 5). Temperatures calculated using the hornblende-plagioclase thermometer of Blundy and Holland (1990) using P1-P4 values are: 776-824ºC (mean= 809 ± 17ºC) for P1, 770-826ºC (mean= 811 ± 17ºC) for P2, 782-830ºC (mean= 815 ± 17ºC) for P3 and 767-815ºC (mean=800 ± 17ºC) for P4 for the Eriko Tepe Pluton (Table 5).

Temperature estimates calculated for the Eriko Tepe Pluton for under <5 kbar pressure are based on the hornblende-plagioclase thermometer of Holland and Blundy (1994) vary between 735-790ºC (mean= 761 ±16ºC) (Table 6a). The pressure and temperature

Table 5- Pressures (P, kbar) calculated according to Hammarstrom and Zen (1986), Hollister et al. (1987), Johnson and Rutherford (1989) and Schmidt (1992) by using hornblendes for the Eriko Tepe and the Göl Tepe Plutons, and the temperatures (T, °C) estimated based on Blundy and Holland (1990) by using these mean pressure values.

	Hammarstrom and Zen (1986) (P1)	**Hollister et al. (1987) (P2)**	**Johnson and Rutherford (1989) (P3)**	**Schmidt (1992) (P4)**
Eriko Tepe Pluton (n=6)				
Max. P (kbar)	1.9	1.4	1.7	2.5
Min. P (kbar)	1.2	0.9	1.0	1.8
Mean P (kbar)	1.5 ± 0.3	1.1 ± 0.3	1.3± 0.4	2.1 ± 0.3
Mean depth (km)	5.6	4.1	4.8	7.8
Blundy and Holland (1990), Hornblende-plagioclase thermometer				
	Hammarstrom and Zen (1986)	**Hollister et al. (1987)**	**Johnson and Rutherford (1989)**	**Schmidt (1992)**
Eriko Tepe Pluton (n=6)	**(P1 =1.5 kbar)**	**(P2 =1.1 kbar)**	**(P2 =1.3 kbar)**	**(P2 =2.1 kbar)**
Max. T (°C)	824	826	830	815
Min. T (°C)	776	778	782	767
Mean T (°C)	809 ± 17	811 ± 17	815 ± 17	800 ± 17

* Depth was taken as 3.7 km for 1 kbar for the continental crust (Tulloch and Callis, 2000).

Table 6- Using the hornblendes for the Eriko Tepe Pluton; a) the temperatures (T, °C) estimated under 5 kbar pressure according to hornblende-plagioclase thermometer of Holland and Blundy (1994), and the temperature (T, °C) and pressure (P, kbar) values estimated based on the hornblende thermobarometer of Ridolfi et al (2010) and Ridolfi and Renzulli (2012); b) the oxygene fugacity [log$f$(O_2)], ΔNNO and H_2O_{melt}(w.%) values calculated based on Wones (1989), Ridolfi et al. (2008 and 2010) and Riddolfi and Renzulli (2012).

a	**Holland and Blundy (1994), Hornblende-plagioclase thermometer (Pressure (P) was taken as 5 kbar in estimations)**	**Ridolfi et al. (2010), Hornblende thermobarometer (calc-alkaline magmas)**		**Ridolfi and Renzulli (2012), Hornblende thermobarometer (calc-alkaline magmas)**	
		Pressure (P, kbar)	**Temperature (T, °C)**	**Pressure (P, kbar)**	**Temperature (T, °C)**
Eriko Tepe Pluton	**(n=13)**	**(n=14)**	**(n=14)**	**(n=14)**	**(n=14)**
Mean T (°C)	761 ± 16	0.8 ± 0.1	781 ± 11	0.9 ± 0.1	746± 19
Max. T (°C)	790	1.0	796	1.1	767
Min. T (°C)	735	0.7	763	0.6	708
b	**Wones (1989)**	**Ridolfi et al. (2008, 2010)**			**Ridolfi and Renzulli (2012)**
	Oxygen fugacity log*f*(O_2)	ΔNNO	**Oxygen fugacity log*f*(O_2)**	**H_2O melt (w.%)**	ΔNNO
Eriko Tepe Pluton	**(n=6)**	**(n=14)**	**(n=14)**	**(n=14)**	**(n=14)**
Mean	-13.6 ± 0.4	1.65 ± 0.36	-12.7 ± 0.4	4.16 ± 0.23	0.90 ± 0.52
Max.	-13.1	2.13	-11.9	4.60	2.14
Min.	-14.4	1.03	-13.4	3.77	0.00

*** Pressure (P, kbar) values used in the oxygen fugacity estimations of Wones (1989) and the temperature (T, °C) values are the calculated values according to Schmidt (1992) and Blundy and Holland (1990), respectively.

estimates based on hornblende, following Ridolfi et al. (2010), vary between 0.7-1.0 kbar (mean= 0.8 ± 0.1 kbar) and 763-796ºC (mean= 781 ± 11ºC), respectively. However, the pressure and temperature values calculated according to Ridolfi and Renzulli (2012) are in between 0.6-1.1 kbar (mean= 0.9 ± 0.1 kbar) and 708-767ºC (mean= 746 ± 19ºC), respectively (Table 6a). The oxygen fugacity values calculated according to Ridolfi et al. (2010) and Wones (1989) using the Mg content of hornblendes in the Eriko Tepe Pluton are, respectively, between (-13.4) - (-11.9) (mean= -12.7 ± 0.4) and (-14.4) - (-13.1) (mean= -13.6 ± 0.4) (Table 6b). However, the ΔNNO values calculated according to Ridolfi et al. (2008, 2010) and Ridolfi and Renzulli (2012) vary between the values of 1.03-2.13 (mean= 1.65 ± 0.36) and 0.00-2.14 (mean= 0.9 ± 0.52), respectively. The H_2O content calculated according to Ridolfi et al. (2008, 2010) varies between the values of 3.77-4.60 (mean= 4.16 ± 0.23) (Table 6b).

The temperature values estimated based on Luhr et al. (1984) and the pressure values calculated according to Uchida et al. (2007) from biotite minerals vary between 730-824ºC (mean= 765 ± 28ºC) and 0.5-1.11 kbar (mean= 0.8 ± 0.15 kbar) for the Eriko Tepe Pluton and 856-1049ºC (mean= 948 ± 52ºC) and 0.54-1.18 kbar (mean= 0.84 ± 0.25 kbar) for the Göl Tepe Pluton (Table 7). The values that are based on the oxygen fugacity model of Wones (1989), using these pressure and temperature values, are between (-15.7) - (-13.1) (mean= -14.7 ± 0.0.8) for the Eriko Tepe Pluton and (-12.3) - (-8.3) (mean= -10.4 ± 1.1) for the Göl Tepe Pluton (Table 7).

Zircon (Miller et al., 2003) and apatite (Harrison and Watson, 1984) saturation temperatures were also calculated using the whole-rock analyses of the Eriko Tepe and the Göl Tepe Plutons. Zircon saturation temperatures (T1 and T2), based on the M and FM parameters of Miller et al. (2003), are between 717-757ºC (mean= 737 ± 16ºC) and 684-734ºC (mean= 708 ± 19ºC) for the Eriko Tepe Pluton and 709-780ºC (mean= 730 ± 24ºC) and 676-766ºC (mean= 703 ± 29ºC) for the Göl Tepe Pluton (Table 8). However, the apatite saturation temperatures, which were calculated

Table 7- The pressure (P, kbar), temperature (T, °C) and oxygene fugacity values calculated according to Luhr et al. (1984), Uchida et al. (2007) and Wones (1989) by using the biotites for the Eriko Tepe and the Göl Tepe Plutons.

	Luhr et al. (1984) Temperature (T, °C)	**Uchida et al. (2007) Pressure (P, kbar)**	**Wones (1989) T and P in (*f*O2) estimations are according to (Luhr et al., 1984) (Uchida et al., 2007), respectively.**
Eriko Tepe Pluton (n=18)			
Mean	765 ± 28	0.80 ± 0.15	-14.7 ± 0.8
Max.	824	1.11	-13.1
Min.	730	0.50	-15.7
Göl Tepe Pluton (n=24)			
Mean	948 ± 52	0.84 ± 0.25	-10.4 ± 1.1
Max.	1049	1.18	-8.3
Min.	856	0.54	-12.3

Table 8- The temperature (T, °C) values estimated for the saturation of zircon (Miller et al., 2003) and apatite (Harrison and Watson, 1984) by using the whole-rock geochemical analyses of the Eriko Tepe and the Göl Tepe Plutons.

	Saturation temperature for Zircon * (Miller et al., 2003)		**Saturation temperature for Apatite (Harrison and Watson, 1984)**
	T1 (M was used)	T2 (FM was used)	
Eriko Tepe Pluton	**(n=18)**	**(n=18)**	**(n=8)**
Mean T (°C)	737 ± 16	708 ± 19	894 ± 9
Max. T (°C)	757	734	908
Min. T (°C)	717	684	883
Göl Tepe Pluton	**(n=7)**	**(n=7)**	**(n=7)**
Mean T (°C)	730 ± 24	703 ± 29	869 ± 18
Max. T (°C)	780	766	898
Min. T (°C)	709	676	845

*Saturation temperatures for zircon (T_1 and T_2) were estimated, by means of the whole-rock geochemical analyses, using the parameters M [=(Na + K + 2Ca)/(Al × Si)] of Watson and Harrison (1983) and FM [=(Na + K + (2Ca + Fe + Mg))/(Al × Si)] of Ryerson and Watson (1987), which are given in Hanchar and Watson (2003), and the experimental models suggested by Miller et al (2003).

based on the formula of Harrison and Watson (1984), are 883-908ºC (mean= 894 ± 9ºC) for the Eriko Tepe Pluton and 845-898ºC (mean= 869 ± 18ºC) for the Göl Tepe Pluton (Table 8).

The crystallization depth corresponding to the mean pressure values (4.8-7.5 kbar) from the clinopyroxene barometry are 17.8-27.8 km. However, the crystallization depth corresponding to the mean pressure values (1.1-2.1 kbar), which had been obtained from the hornblende barometry, were detected as 4.1-7.8 km (1 kbar= 3.7 km for the continental crust; Tulloch and Challis, 2000). So, this indicates that these plutonic rocks were subjected to early stage high pressure and late stage low pressure polybaric crystallization at mid to shallow crustal depths. The oxygen fugacity values calculated from the hornblendes and biotites are close to, or just in, the upper part of the NiNiO buffer zone and the plutons are the products of the similar magmas.

7.2. Origin of the Parental Magmas

There are many petrogenetical models related to the origins of granitic-monzonitic magmas: (1) fractional crystallization (FC) and/or assimilation+fractional crystallization (AFC) from mantle derived basaltic parental magmas (Grove and Donnelly-Nolan, 1986; Bacon and Druitt, 1988; Rapela and Pankhurst, 1996; Soesoo, 2000; Jiang et al., 2002; Liu et al., 2008; Li et al., 2009; Aghazadeh et al., 2010, 2011); (2) the partial melting of mafic to intermediate meta-magmatic crustal rocks (Roberts and Clemens, 1993; Xu et al., 2004; Köksal et al., 2013); (3) the mixing of mantle derived mafic magma and crustal origin felsic magmas (Neves and Mariano, 1997; Ferré et al., 1998; Barbarin, 1999; Gagnevin et al., 2004; Yang et al., 2007, 2011; Ackerman et al., 2010; Lan et al., 2011, 2012, 2013; Cheng et al., 2012; Donskaya et al., 2013; Mao et al., 2013; Wang et al., 2013; Liu et al., 2013, 2014), and, (4) the partial melting of felsic magmas, mafic to intermediate meta magmatic (Rapp and Watson, 1995; Singh and Johannes, 1996) or meta-sedimentary (Patiño Douce and Beard, 1996; Stevens et al., 1997) rocks based on the principle that mantle derived basaltic magmas provide heat to melt crustal rocks (Bullen and Clynne, 1990; Roberts and Clemens, 1993; Guffanti et al., 1996). It is also known that the shoshonitic magmas generally form in the arc and post-collisional environments (eg, Foley and Peccerillo, 1992; Turner et al., 1996). It is also asserted that the shoshonitic magmas, which were formed in the post-collisional environments, had been derived from: (i) the peridotite-amphibolite-metapelite mixture on the crust-mantle boundary (López-Moro and López-Plaza, 2004); (ii) the mixture of asthenospheric and enriched lithospheric mantle (Li et al. 2000), and, (iii) the mantle metasomatism of which the subducted sediments had caused or the enriched lithospheric mantle (Turner et al., 1996; Wang et al., 1996; Eklund et al., 1998; Liu et al., 2002).

The monzonitic rocks, which form the Eriko Tepe Pluton (SiO_2: 56-59 % and Mg#: 29-33) and the Göl Tepe Pluton (SiO_2: 53-64 %, Mg#: 26-31), are I-type, metaluminous (Eriko Tepe Pluton; A/CNK=0.78-0.89 and Göl Tepe Pluton; A/CNK=0.76-0.93) and shoshonitic and possess molar K_2O/Na_2O, molar CaO/(MgO+Fe_2O_3*) and A/CNK ratios varying mainly in a narrow interval (Figure 11a, b). In terms of Th/U vs U (ppm) they plot in the areas which show that the melts are derived from the middle-lower continental crust (Figure 11c). In terms of La/Yb vs Nb/La they plot on the lithospheric mantle and in the area close to the intermediate continental crust composite in the diagram (Figure 11d). However, in terms of La/Nb vs Ba/Nb (Figure 11e) and Nb (ppm) vs Nb/Th (Figure 11f), the monzonitic rocks plot on the area of arc volcanics they show a tendency for subduction enrichment. When the major molar and trace element ratio diagrams are assessed together, it is apparent that the parental magmas of the monzonitic plutons may be derived from the decompressional melting of lithospheric mantle that is enriched by different ratios of amphibole and plagioclase in different H_2O contents.

These monzonitic rocks have negative Nb and TiO_2 anomalies and Sr, Rb, K_2O, Th, Ce and La enrichments in the primitive mantle-normalized diagrams. They also indicate that parental magmas of these plutons might have been derived from the mixtures of lithospheric mantle enriched by previous subduction events and that the continental crust melts in fewer ratios. However, low-intermediate Rb/Sr ratios (0.13-0.35), intermediate-high K_2O (3.9-5.2%) and SiO_2 (53-64%) contents show that the parental magmas of these rocks may have been derived from the much enriched lithospheric mantle source (Jung et al., 2009). The trace element variations of monzonitic plutons with high LILE/HFSE ratios and their REE distributions with slightly moderate degree enrichments (Eriko Tepe Pluton: La_N/Lu_N=9.26-10.68; Göl Tepe Pluton: La_N/Lu_N= 9.72-12.57) show similarity to each other.

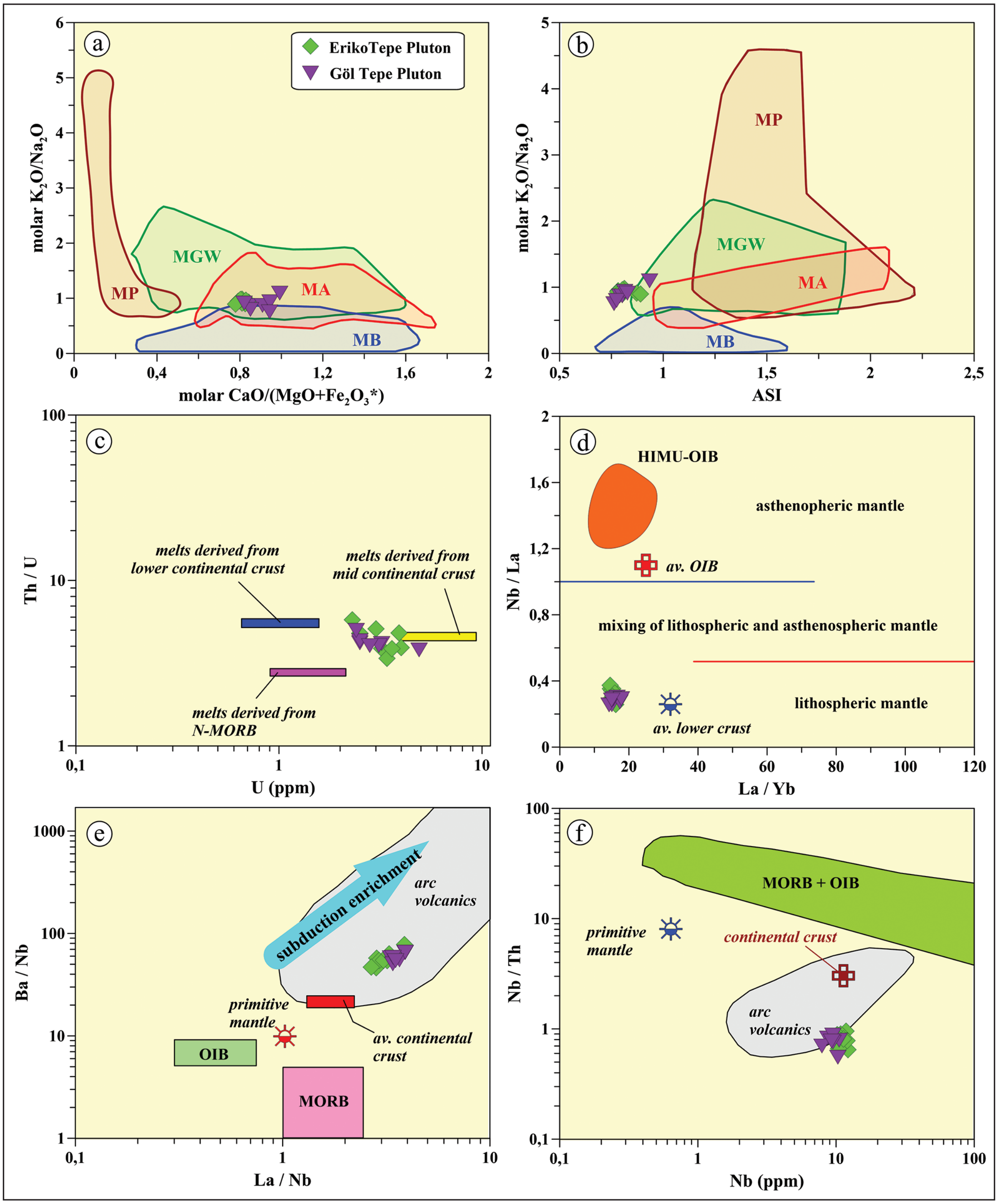

Figure 11- (a) The molar K_2O/Na_2O vs molar $CaO/(MgO+Fe_2O_3*)$, (b) molar K_2O/Na_2O vs ASI (A/CNK), (c) U (ppm) vs Th/U, (d) La/Yb vs Nb/La, (e) La/Nb vs Ba/Nb and (f) Nb (ppm) vs Nb/Th plots for the rocks of the Eriko Tepe and the Göl Tepe Plutons. The data for (a) and (b); MB: metabasalt, MA: metaandesite; MGW: metagreywacke, MP: metapelite. The fields are based on Vielzeuf and Holloway (1988), Patiño Douce and Johnston (1991), Rapp et al. (1991), Gardien et al. (1995), Rapp (1995), Rapp and Watson (1995), Patiño Douce and Beard (1996), Stevens et al. (1997), Skjerlie and Johnston (1996), Patiño Douce (1997), Patiño Douce and McCarthy (1998), Patiño Douce (1999). (c); the field belonging to the lower and intermediate continental crust and the depleted Mid Oceanic Ridge Basalt (MORB) area from Rudnick and Gao (2003) and Sun et al. (2008), respectively. (d); the boundaries among the atmospheric mantle, lithospheric mantle and the mixture of lithospheric–atmospheric mantles from Smith et al. (1999), the HIMU-OIB (Oceanic Island Basalt) area from Weaver et al. (1987), the mean OIB value from Fitton et al. (1991) and the mean lower crust value from Chen and Arculus (1995). (e); the arc volcanic field from Jahn and Zhang (1984), the primitive mantle value from Sun and McDonough (1989), the mean continental crust value from Taylor and McLennan (1985) and Condie (1993), and fields of MORB and OIB from Le Roex (1987). (f); the primitive mantle value from Hofmann (1988), continental crust value and fields of MORB, OIB and arc volcanics from Schmidberger and Hegner (1999).

It emphasizes that parental magmas of these plutons have been derived from the similar sources and through similar magmatic processes (differentiation and crust assimilation).

7.3. Fractional Crystallization (FC) and Assimilation-Fractional Crystallization (AFC)

The correlations (see Figures 8 and 9), which are observed in some major oxide and trace element variations in the Harker diagrams for monzonitic rocks of the Eriko Tepe and Göl Tepe Plutons, show that the FC is significant in the evolution of these plutons. There is a positive correlation between the SiO_2 and the K_2O, Nb, Ba, Hf, Th and Ta contents, however, there is a negative correlation between the SiO_2 content and TiO_2, Fe_2O_3*, MgO, MnO, CaO, P_2O_5 and Sr contents in monzonitic rocks of the Eriko Tepe and the Göl Tepe Plutons (see Figures 8 and 9). Generally the decrease of Fe_2O_3* indicates clinopyroxene fractionation. Nevertheless, the decrease of CaO with increasing SiO_2 indicates clinopyroxene and plagioclase fractionation. The decrease in Sr, but increase in K_2O, with respect to the increase in SiO_2, indicates K-feldspar fractionation. The decrease in P_2O_5, TiO_2 and Sr with the increase in SiO_2 indicates that apatite, magnetite and plagioclase fractionated, however, the decrease in Fe_2O_3*, MgO and MnO indicate that hornblende and biotite fractionated. In general, K_2O, showing a positive correlation with SiO_2, emphasizes biotite and K-feldspar fractionations. The studied plutons exhibit a concave shaped pattern in REE distributions, verifying the effectiveness of clinopyroxene and/or hornblende fractionations in their evolution (Thrilwall et al., 1994). Besides; the weak negative Eu anomaly observed in monzonitic rocks of the Eriko Tepe Pluton (Eu_N/Eu^*: 0.69-0.84) and the Göl Tepe Pluton (Eu_N/Eu^*: 0.72-0.82) indicates that K-feldspar±plagioclase fractionation is effective in the evolution of these rocks (see Figure 10 b).

The irregular correlations observed in some major oxide and trace element variations (see Figures 8 and 9) could also indicate crustal assimilation ± magma mixing in addition to the fractional crystallization. The correlations observed in MgO (%)-Sr (ppm) and Rb (ppm)-K_2O/Rb diagrams (Figure 12a, b) that plagioclase, K-feldspar, clinopyroxene, hornblende, biotite and Fe-Ti oxide all fractionated in the evolution of the plutons. However, the contribution of continental crust in the evolution of the plutons can be clarified by Ta/Yb vs Th/Yb diagrams (Figure 12c) (Pearce, 1983). In this diagram, the plutonic rock samples examined show a tendency towards the average continental crust value with high Th/Yb and Ta/Yb ratios (Figure 12c). Accordingly it is possible to say that the AFC has also played a lesser role compared to FC in the evolution of these plutons (Figure 12c). The AFC modelling was

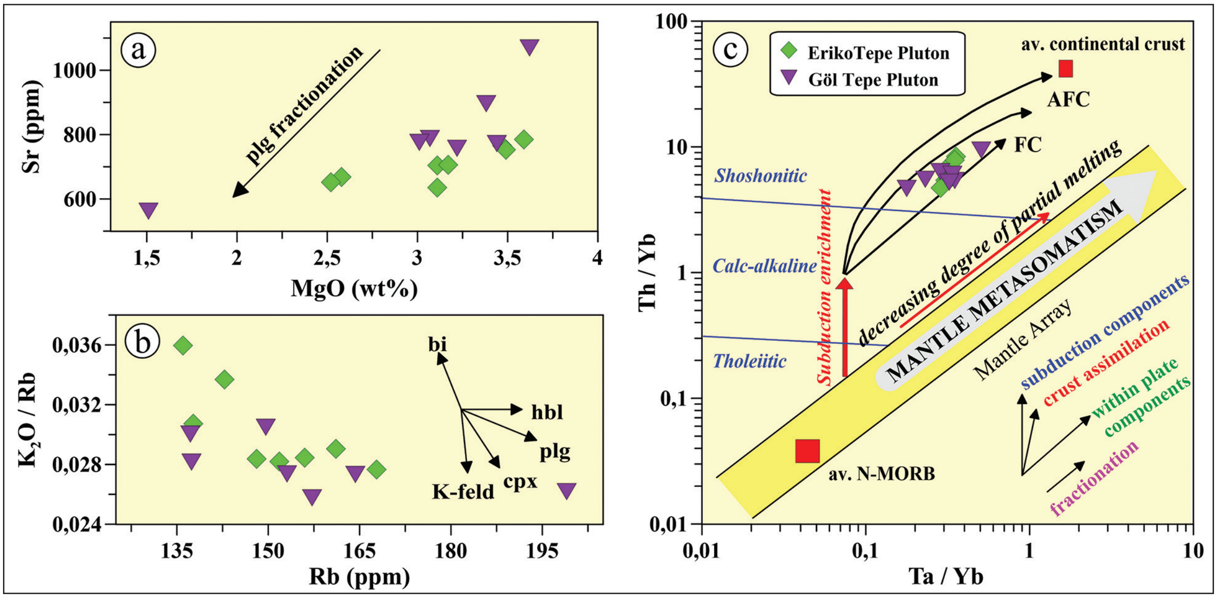

Figure 12- The plots of; a) MgO (wt%) vs Sr (ppm), b) Rb (ppm) vs K_2O/Rb and c) Ta/Yb vs Th/Yb (Pearce, 1983) (pl: plagioclase, cpx: clinopyroxene, hb: hornblende, bi: biotite, K-feld: K-feldspar) show directions of FC (fractional crystallization) and/or AFC (assimilation+fractional crystallization) and the mineral fractionation for the rocks of the Eriko Tepe and the Göl Tepe Plutons. The vectors showing FC, AFC, subduction enrichment and the mantle metasomatism were taken from Pearce et al. (1990).

based on trace element contents and/or ratios (Figures 13a, b and c) (DePaolo, 1981; Powell, 1984). All samples in diagrams of La-Nb and La-La/Nb (Figures 13a, b), which show the AFC of monzonitic rocks, plot on or near the r=0.2 curve. However, they plot on or near the r=0.05 curve in the Zr-Zr/Nb diagram (Figure 13c). Generally the r value is less than or equal to 0.2, less than the critical value of r=0.25 (Albarède, 1996) shows that FC is more effective than AFC in the evolution of these monzonitic rocks.

7.4. Magma-Tectonic Environment of Plutons

The different magma-tectonic evolution models for the Tertiary magmatism in the Eastern Pontides are suggested to be: (1) the slab-break off of the subduction plate (Boztuğ et al., 2004, 2006); (2) the southward roll-back and synchronous slab-window (Eyüboğlu et al., 2011*a, b, c*), and, (3) the lithospheric delamination (Karslı et al., 2007, 2010*b*, 2012*b*; Temizel et al., 2012*a*; Arslan et al., 2013*a*). When the geochemical and petrological characteristics of Eocene (~ 45-40 Ma) intermediate-high K and shoshonitic volcanic rocks (eg. Arslan and Aliyazıcıoğlu, 2001; Temizel et al., 2012*a*; Arslan et al., 2013*a*; Temizel et al., 2016; Yücel et al., 2017) and I-type, metaluminous and shoshonitic plutonic rocks (eg. Boztuğ et al., 2004; Boztuğ and Harlavan, 2008; Topuz et al., 2005; 2011; Arslan and Aslan, 2006; Karslı et al., 2007, 2010*a*, 2011, 2012*b*) were considered, it was asserted that the magmatism is characterized by the extensional tectonic setting related with the crustal thickening and lithospheric detachment, and has derived mainly from enriched sub-continental lithospheric mantle and lower continental crust melts and/or mixtures (Temizel et al., 2012*a*; Arslan et al. 2013*a*; Aslan et al., 2014; Yücel et al., 2017).

In order to determine the magma-tectonic environments of the monzonitic plutons, the

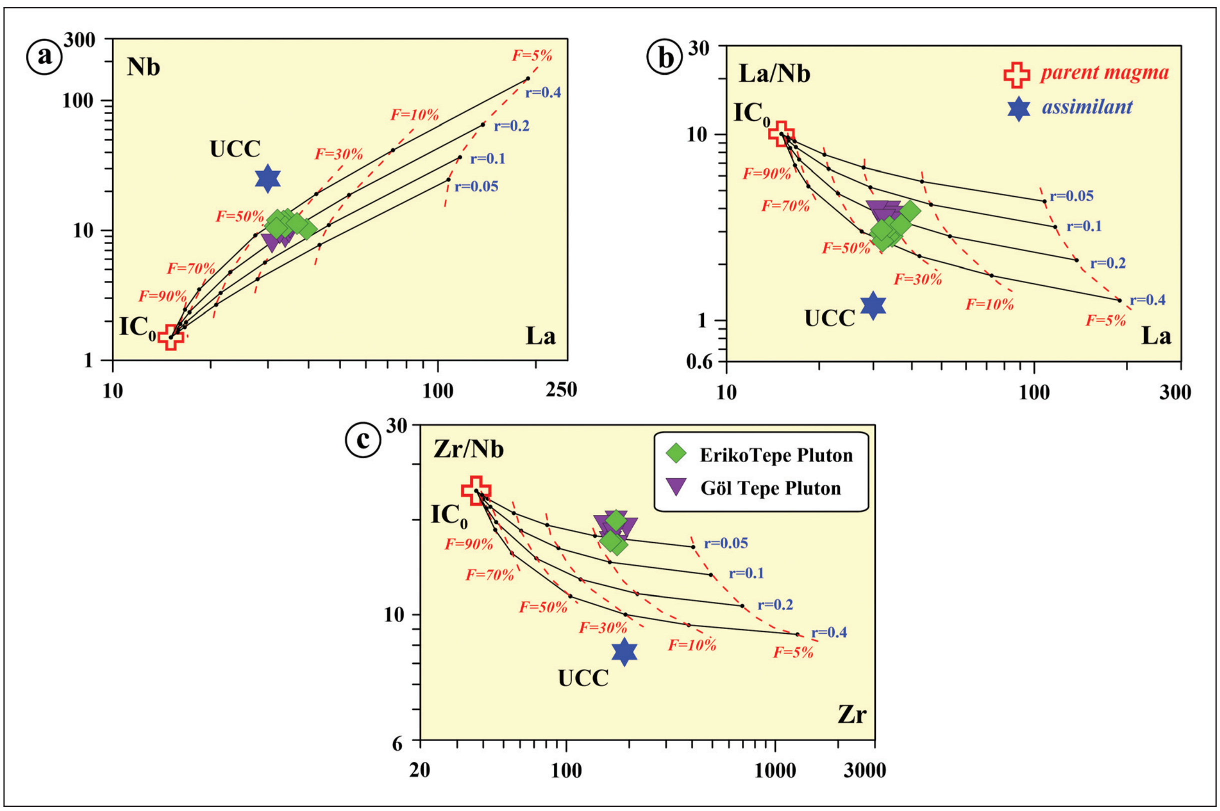

Figure 13- The plots of; a) Nb (ppm) vs La (ppm), b) La/Nb vs La (ppm) and c) Zr/Nb vs Zr (ppm), which show the trace element AFC modelling in the rocks of the Eriko Tepe and the Göl Tepe Plutons. Parental magma composition (IC_0; La = 15.1 ppm, Zr = 37.1 ppm and Nb = 1.5 ppm; CIPW mineralogy = olivine: 17.38, clinopyroxene: 17.83, plagioclase: 45.85, magnetite: 3.52) is the basalt sample SIR-108 from Arslan et al. (2013*a*). The Upper Continental Crust composition as the assimilant (La = 30 ppm, Zr = 190 ppm and Nb = 25 ppm) from Taylor and McLennan (1985) and the portition coefficients from McKenzie and O'Nions (1991). The AFC curves were drawn based on different r values (ratio of the fractional crystallization with respect to assimilation; 0.05, 0.1, 0.2 and 0.4) and the values of different F (fractionation degrees (%); 5, 10, 30, 50, 70, 90).

discrimination diagrams for the plutonic rocks were used. According to Rb-(Y+Nb) and Ta-Yb diagrams of Pearce et al. (1984) (Figure 14a, b) the samples belonging to the studied plutons plot on areas of volcanic arc and post-collisional granites. Further, they plot on fields of arc granites and granites formed by the collisional tectonics according to the Rb/10-Hf-Ta*3 ternary diagram of Harris et al. (1986) (Figure 14c), and magmatic or crust origin due to the interaction of mantle-crust (Figure 14d). Thus, considering other geological and geochemical data, it can be asserted that the studied plutons has formed from the lithospheric mantle derived magmas (with less amount of continental crust assimilation) in the Eocene post collisional environment in the Eastern Pontides.

8. Conclusions

The Eriko Tepe and Göl Tepe plutons outcropping in the southeastern part of the Gölköy (Ordu) area in the Eastern Pontides Orogenic Belt were formed from mainly monzonitic and rarely quartz-monzonitic and monzodioritic rocks in composition.

The plutons both have similar mineralogical and textural characteristics, only the Eriko Tepe pluton consists of magnesio-hornblende different than the Göl Tepe pluton. There were also observed some textural features in these studied plutons indicating disequilibrium crystallization, such as: the corrosion of clinopyroxene, the poikilitic textures observed in K-feldspars minerals and clinopyroxene minerals surrounded by the biotite minerals.

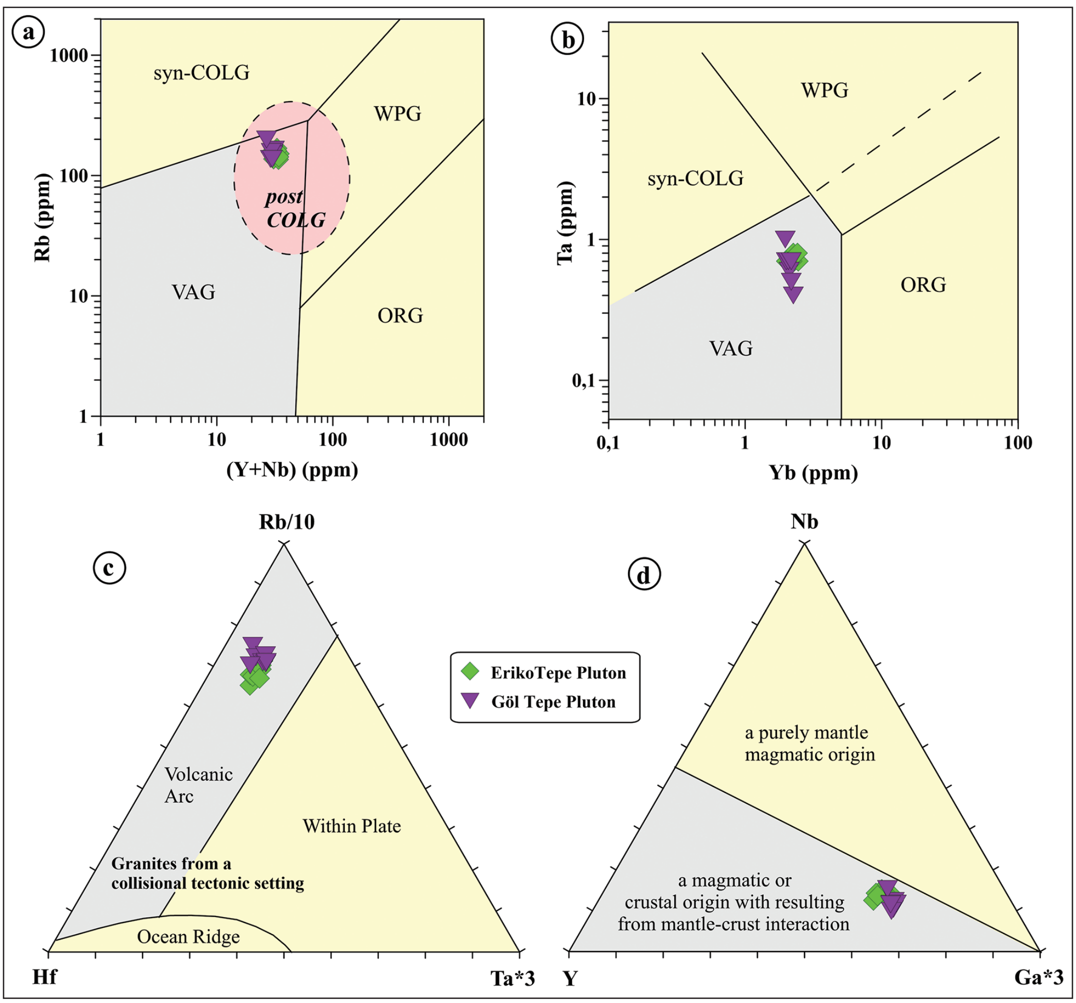

Figure 14- The magma-tectonic discrimination plots of the rocks from the Eriko Tepe and the Göl Tepe Plutons; a) Rb (ppm) vs (Y+Nb) (ppm), b) Ta (ppm) vs Yb (ppm), c) Rb/10-Hf-Ta*3 (Harris et al., 1986) and d) Nb-Y-Ga*3 (Eby, 1992) ternary diagrams. Syn-COLG: Syn-collisional granites, VAG: Volcanic Arc Granites; WPG: Within Plate Granites; ORG: Oceanic Ridge Granites; post-COLG: Post-collisional Granites.

The P-T conditions were detected by means of the chemistry of feldspar, clinopyroxene, hornblende and biotite minerals in the studied plutons. The calculated temperature and pressure values vary between 684-726ºC for feldspars, 1119-1158ºC and 4.8-7.5 kbar for clinopyroxenes, 1.1-2.1 kbar and 761-815ºC for hornblendes and 765-948ºC and 0.80-0.84 kbar for biotites. This indicates that the plutons were generally crystallized at mid to shallow crustal depths.

The whole-rock geochemical data show that the studied plutons are I-type, metaluminous and shoshonitic in character. The major and trace element variations indicate that the plutons were differantiated significantly by fractional crystallization and lesser crustal assimilation during the evolution of the magma chamber in the continental crustal.

It can be asserted that the parental magmas were derived from the enriched lithospheric mantle by decompressional melting in a post-collisional setting.

Acknowledgements

This study has been supported by the TÜBİTAK-ÇAYDAG project, number 113Y404. The authors thank to Prof. Nurdane İlbeyli and Assoc. Prof. Fuat Erkül for their constructive critiques and suggestions. We are also grateful to Dr. Sarah Sherlock for reviweving and editing of the English version.

Supplementary Data

Tables 1-5; Electronic Data for Appendices are available at https://dergi.mta.gov.tr/documents/1991_157_supplementary_tables_irfan_temizel.pdf

References

Ackerman, L., Krňanská, M., Siebel, W., Strnad, L. 2010. Geochemistry of the Drahotín and Mutěnín intrusions, West Bohemian shear zone, Bohemian massif: contrasting evolution of mantle-derived melts. Mineralogy and Petrology 99, 185-199.

Aghazadeh, M., Castro, A., Omran, N.R., Emami, M.H., Moinvaziri, H., Badrzadeh, Z. 2010. The gabbro (shoshonitic)–monzonite–granodiorite association of Khankandi pluton, Alborz Mountains, NW Iran. Journal of Asian Earth Sciences 38, 199-219.

Aghazadeh, M., Castro, A., Badrzadeh, Z., Vogt, K. 2011. Post-collisional polycyclic plutonism from the Zagros hinterland. The Shaivar-Dagh plutonic complex Alborz belt, Iran. Geological Magazine 148, 980-1008.

Ağar, U. 1977. Demirözü (Bayburt) ve Köse (Kelkit) Bölgesinin Jeolojisi. Doktora Tezi, İstanbul Üniversitesi, İstanbul (unpublished).

Albaréde, F. 1996. High-resolution geochemical stratigraphy of Mauna Kea flows from the Hawaii Scientific Drilling Project core. Journal of Geophysical Research. Solid Earth.

Aliyazıcıoğlu, İ. 1999. Kale (Gümüşhane) yöresi volkanik kayaçlarının petrografi, jeokimyasal ve petrolojik incelenmesi. Yüksek Lisans Tezi, KTÜ Fen Bilimleri Enstitüsü, 96 s. Trabzon (unpublished).

Altherr, R., Topuz, G., Siebel,W., Şen, C., Meyer, H.P., Satır, M. 2008. Geochemical and Sr-Nd-Pb isotopic characteristics of Paleocene plagioleucitites from the Eastern Pontides (NE Turkey). Lithos,105, 149-161.

Arslan, M., Aliyazıcıoğlu, İ. 2001. Geochemical and petrological characteristics of the Kale (Gümüşhane) volcanic rocks: implications for the Eocene evolution of eastern Pontide arc volcanism, northeast Turkey. International Geology Review 43, 7, 595-610.

Arslan, M., Aslan, Z. 2006. Mineralogy, petrography and whole-rock geochemistry of the Tertiary granitic intrusions in the eastern Pontides, Turkey. Journal of Asian Earth Sciences 27, 177-193.

Arslan, M., Tüysüz, N., Korkmaz, S., Kurt, H. 1997. Geochemistry and Petrogenesis of the Eastern Pontide Volcanic Rocks, Northeast Turkey. Chemi der Erde 57, 157-187.

Arslan, M., Temizel, İ., Abdioğlu, E. 2002. Subduction input versus source enrichment and role of crustal thickening in the generation of Tertiary magmatism in the Pontid Paleo-Arc setting, NE Turkey. In: De Vivo, B., R. J. Bodgar, R. J. (Eds.) Workshop-Short Course on Volcanic Systems, Geochemical and Geophysical Monitoring, Melt inclusions: Methods, applications and problems, 13-16, Napoli, Italy.

Arslan, M., Temizel, İ., Abdioğlu, E., Kolaylı, H., Yücel, C., Boztuğ, D., Şen, C. 2013*a*. ^{40}Ar-^{39}Ar dating, whole-rock and Sr-Nd-Pb isotope geochemistry of post-collisional Eocene volcanic rocks in the southern part of the Eastern Pontides (NE Turkey): Implications for magma evolution in extension-induced origin. Contribution to Mineralogy and Petrology 166, 113-142.

Arslan, M., Abdioğlu, E., Temizel, İ., Yücel, C. 2013*b*. Doğu Pontid Kuzey Zonu Tersiyer volkanitlerinin petrokimyası, Sr-Nd-Pb izotop jeokimyası, jeokronolojisi ve jeodinamik gelişimi. TÜBİTAK ÇAYDAG Projesi No: 108Y204.

Aslan, Z., 2010. U-Pb zircon SHRIMP age, geochemical and petrographical characteristics of tuffs within calc-alkaline Eocene volcanics around Gümüşhane (NE Turkey), Eastern Pontides. Neues Jahrbuch für Mineralogie Abhandlungen 187, 329-346.

Aslan, Z., Arslan M., Şen, C. 1999. Doğu Pontidlerin Kuzey ve Güney zonlarında yüzeylenen Eosen yaşlı granitik sokulumların karşılaştırmalı jeolojik, petrografik ve jeokimyasal özellikleri. Türkiye Jeoloji Kurultayı Bildiriler Kitabı, 223-230.

Aslan, Z., Arslan, M., Temizel, İ., Kaygusuz, A. 2014. K-Ar dating, whole-rock and Sr-Nd isotope geochemistry of calc-alkaline volcanic rocks around the Gümüşhane area: implications for post-collisional volcanism in the Eastern Pontides, Northeast Turkey. Mineralogy and Petrology 108, 245-267.

Aydın, F., Karslı, O., Chen, B. 2008. Petrogenesis of the Neogene alkaline volcanics with implications for post collisional lithospheric thinning of the Eastern Pontides, NE Turkey. Lithos 104, 249-266.

Aydın, F., Thompson, R., Karsli, O., Uchida, H., Burt, J.B., Downs, R.T. 2009. C2/c pyroxene phenocrysts from there potassic series in Neogene alkaline volcanics, Ne Turkey: Their crystal chemistry with petrogenetic significance as an indicator of P-T conditions. Contributions to Mineralogy and Petrology 158, 131-147.

Bacon, C.R., Druitt, T.H. 1988. Compositional Evolution of the Zoned Calc-Alkaline Magma Chamber of Mount Mazama, Crater Lake, Oregon. Contribution to Mineralogy and Petrology 98, 224-256.

Barbarin, B. 1999. A review of relationships between granitoid types, their origins and their geodynamic environments. Lithos 46, 605-626.

Bektaş, O., Pelin, S., Korkmaz, S. 1984. Doğu Pontid yay gerisi havzasında manto yükselimi ve polijenetik ofiyolit olgusu. TJK Ketin Sempozyumu, pp. 175-188.

Bektaş, O., Şen, C., Atıcı, Y., Köprübaşı, N. 1999. Migration of the Upper Cretaceous subduction-related volcanism towards the back-arc basin of the Eastern Pontide magmatic arc (NE Turkey). Geological Journal 34, 95-106.

Blundy, J.D., Holland, T.J. B. 1990. Calcic amphibole equilibria and a new amphibole-plagioclase geothermometer. Contributions to Mineralogy and Petrology 104, 208-224.

Boztuğ, D., Harlavan, Y. 2008. K-Ar ages of granitoids unravel the stages of Neo-Tethyan convergence in the eastern Pontides and central Anatolia, Turkey. International Journal of Earth Sciences 15, 585-599.

Boztuğ, D., Avcı, N., Tatar, S., Zorlu, M., Tüvar, O. 2003. Mineralogical and geochemical evidences of the interaction between co-eval mafic and felsic magma sources in the genesis of the A-type Murmana and Dumluca granitoids, Divriği SE Sivas, Central Turkey. International Conference The South Aegean Active Volcanic Arc: Present Knowledge and Future Perspectives. SAAVA-2003, Milos Island, Greece, Book of Abstracts, 43-44.

Boztuğ, D., Jonckheere R., Wagner, G. A., Yeğingil, Z. 2004. Slow Senonian and fast Palaeocene-Early Eaocene uplift of the granitoids in the central eastern Pontides, Turkey: apatite fission-track results. Tectonophysics 382, 213-228.

Boztuğ, D., Erçin, A.İ., Kuruçelik, M.K., Göç, D., Kömür, İ., İskenderoğlu, A. 2006. Geochemical characteristics of the composite Kaçkar batholith generated in a Neo-Tethyan convergence system, Eastern Pontides, Turkey. Journal of Asian Earth Sciences 27, 286-302.

Bullen, T.D., Clynne, M.A., 1990. Trace Element and Isotopic Constraints on Magmatic Evolution at Lassen Volcanic Center. Journal of Geophysic Research 95, 19671-19691.

Chen, W., Arculus, R.J. 1995. Geochemical and isotopic characteristics of lower crustal xenoliths, San Francisco Volcanic Field, Arizona, U.S.A. Lithos 110, 99-119.

Cheng, Y.B., Spandler, C., Mao, J.W., Rusk, B.G. 2012. Granite, gabbro and mafic microgranular enclaves in the Gejiu area, Yunnan Province, China: a case of twostage mixing of crust- and mantle-derived magmas. Contributions to Mineralogy and Petrology 164, 659-676.

Chorowicz, J., Collet, B., Bonavia, F., Mohr, P., Parrot, J.F., Tesfaye, K. 1998. The Tana basin, Ethiopia: Intra-plateau uplift, rifting and subsidence. Tectonophysics 295, 351-367.

Condie, K.C. 1993. Chemical composition and evolution of the upper continental crust: contrasting results from surface samples and shales. Chemical Geology 104, 1-37.

Çoğulu, E. 1975. Gümüşhane ve Rize Granitik Plütonlarnın Mukayeseli Petrojeolojik ve Jeokronometrik Etüdü. Doçençtlik Tezi, İTÜ. Maden Fakültesi, İstanbul (unpublished).

Deer, W.A., Howie, R.A., Zussman, J. 1992. An introduction to the Rock Forming Minerals (second edition), London, Longman, 696 s.

DePaolo, D.J., 1981. Trace element and isotopic effects of combined wall-rocks assimilation and fractional crystallization. Earth and Planetary Science Letters 53, 189-202.

Dewey, J.F., Pitman, W., Ryan, W., Bonnin, I. 1973. Plate tectonics and the evolution of the Alpine system, Geological Society American Bulletin 84, 3137-3180.

Dilek, Y. 2006. Collision tectonics of the Eastern Mediterranean region: Causes and consequences. Geological Society of America Special Paper 409, 1-13.

Dilek, Y., Sandvol, E. 2009. Seismic structure, crustal architecture and tectonic evolution of the Anatolian-African plate boundary and the Cenozoic orogenic belts in the eastern Mediterranean region. In Murphy, J. B., Keppie, J. D., Hynes, A. J. (eds.), Ancient orogens and modern analogues, Geological Society of London. Special Publications 327, 127-160.

Dilek, Y., Imamverdiyev, N., Altunkaynak, S. 2010. Geochemistry and tectonics of Cenozoic volcanism in the Lesser Caucasus (Azerbaijan) and the peri-Arabian region: Collision-induced mantle dynamics and its magmatic fingerprint. International Geology Review 52, 4–6, 536-578.

Dokuz, A. 2011. Slab Detachment and Delamination Model for the Generation of Carboniferous High-Potassium I-type Magmatism in the Eastern Pontides, NE Turkey: The Köse Composite Pluton. Gondwana Research 19, 926-944.

Dokuz, A., Tanyolu, E. 2006. Geochemical constraints on the provenance, mineral sorting and subaerial weathering of lower Jurassic and upper Cretaceous clastic rocks from the Eastern Pontides, Yusufeli (Artvin), NE Turkey. Turkish Journal of Earth Sciences 15, 181-209.

Dokuz, A., Karslı, O., Chen, B., Uysal, İ. 2010. Sources and petrogenesis of Jurassic granitoids in the Yusufeli area, Northeastern Turkey: Implications for pre- and postcollisional lithospheric thinning of the Eastern Pontides. Tectonophysics 480, 259-279.

Donskaya, T.V., Gladkochub, D.P., Mazukabzov, A.M., Ivanov, A.V. 2013. Late Paleozoic–Mesozoic subduction-related magmatism at the southern margin of the Siberian continent and the 150 million-year history of the Mongol-Okhotsk Ocean. Journal of Asian Earth Sciences 62, 79-97.

Eby, G.N. 1992. Chemical subdivision of the A-type granitoids: petrogenetic and tectonic implications. Geology 20, 641-644.

Eklund, O., Konopelko, D., Rutanen, H., Fröjdö, S., Shebanov, A.D. 1998. 1.8 Ga Svecofennian post-collisional shoshonitic magmatism in the Fennoscandian shield. Lithos 45, 87-108.

Eyüboğlu, Y., Chung, S.L., Dudas, F.O., Santosh, M., Akaryali, E. 2011*a*. Transition from shoshonitic to adakitic magmatism in the eastern Pontides, NE Turkey: implications for slab window melting. Gondwana Research 19, 413-429.

Eyüboğlu, Y., Santosh, M., Chung, S.L. 2011*b*. Crystal fractionation of adakitic magmas in the crust-mantle transition zone: petrology, geochemistry and U-Pb zircon chronology of the Seme adakites, eastern Pontides, NE Turkey. Lithos 121, 151-166.

Eyüboğlu, Y., Santosh, M., Chung, S.L. 2011c. Petrochemistry and U-Pb zircon ages of adakitic intrusions from the Pulur Massif (Eastern Pontides, NE Turkey): Implications for slab rollback and ridge subduction associated with Cenozoic convergent tectonics in the Eastern Mediterranean. Journal of Geology 119, 394–417.

Eyüboğlu, Y., Santosh, M., Yi, K., Bektaş, O., Kwon, S. 2012. Discovery of Miocene adakitic dacite from the Eastern Pontides Belt and revised geodynamic model for the late Cenozoic Evolution of eastern Mediterranean region. Lithos 146-147, 218-232.

Eyüboğlu, Y., Santosh, M., Dudas, F.O., Akaryali, E., Chung, S.L., Akdağ, K., Bektaş, O. 2013*a*. The nature of transition from adakitic to non-adakitic magmatism in a slab-window setting: a synthesis from the eastern Pontides, NE Turkey. Geosciences Frontiers 4, 353-375.

Eyüboğlu, Y., Dudas, F.O., Santosh, M., Yi, K., Kwon, S., Akaryali, E. 2013*b*. Petrogenesis and U–Pb zircon chronology of adakitic porphyries within the Kop ultramafic masif (Eastern Pontides Orogenic Belt, NE Turkey). Gondwana Research 24, 742-766.

Eyüboğlu, Y., Dudas, F.O., Santosh, M., Zhuc, D.C., Yi, K., Chatterjee, N., Jeong, Y.J., Akaryalı, E., Liuc, Z. 2016. Cenozoic forearc gabbros from the northern zone of the Eastern Pontides Orogenic Belt, NE Turkey: Implications for slab window magmatism and convergent margin tectonics. Gondwana Research 33, 160-189.

Ferré, E.C., Caby, R., Peucat, J.J., Capdevila, R., Monié, P. 1998. Pan-African, postcollisional, ferro-potassic granite and quartz–monzonite plutons of Eastern Nigeria. Lithos 45, 255-279.

Fitton, J.G., James, D., Leeman, W.P. 1991. Basic magmatism associated with late Cenozoic extension in the western United States: Compositional variations in space and time. Journal of Geophysical Research 96, 13693-13711.

Foley, S., Peccerillo, A. 1992. Potassic and ultrapotassic magmas and their origin. Lithos 28, 181–185.

Gagnevin, D., Daly, J.S., Poli, G. 2004. Petrographic, geochemical and isotopic constraints on magma dynamics and mixing in the Miocene Monte Capanne monzogranite (Elba Island, Italy). Lithos 78, 1-2, 157-195.

Gardien, V., Thompson, A.B., Grujic, D., Ulmer, P. 1995. Experimental Melting Of Biotite + Plagioclase + Quartz ± Muscovite Assemblages and Implications for Crustal Melting. Journal of Geophysical Research 100, 15581-15591.

Grove, T.L., Donnelly-Nolan, J.M. 1986. The Evolution of Young Silicic Lavas at Medicine Lake Volcano, California: Implications for the Origin of Compositional Gaps in Calc-Alkaline Series Lavas. Contributions to Mineralogy and Petrology 92, 281-302.

Guffanti, M., Clynne, M. A., Muffler, L.J.P. 1996. Thermal and Mass İmplications of Magmatic Evolution in the Lassen Volcanic Region, California, and Constraints on Basalt Influx to the Lower Crust. Journal of Geophysical Research 101, 3001-3013.

Güven, İ.H. 1993. Doğu Pontidler'in 1/250000 Ölçekli Kompilasyonu, Maden Tetkik ve Arama Genel Müdürlüğü, Ankara.

Hammarstrom, J.M., Zen, E. 1986. Aluminum in hornblende: An empirical igneous geobarometer. American Mineralogist 71, 1297-1313.

Hanchar, J.M., Watson, E.B. 2003. Zircon saturation thermometry. Reviews in Mineralogy and Geochemistry 53, 1, 89-112.

Harris, N. B. W., Pearce, J., Tindle, A.G. 1986. Geochemical characteristics of collision zone magmatism. Collision Tectonic. Geology Society of American Bulletin . Special Pub. No: 19:67-81.

Harrison, T.M., Watson, E.B. 1984. The behaviour of apatite during crustal anatexis: equilibrium and kinetic considerations. Geochimica et Cosmochimica Acta 48, 1467-1477.

Hastie, A.R., Kerr, A.C., Pearce, J.A., Mitchell, S.F. 2007. Classification of Altered Volcanic Island Arc Rocks using Immobile Trace Elements: Development of the Th-Co Discrimination Diagram. Journal of Petrology 48, 12, 2341-2357.

Hofmann, A.W. 1988. Chemical differentiation of the Earth: the relationship between mantle, continental crust, and oceanic crust. Earth and Planetary Science Letters 90, 297-314.

Holland, T.J.B., Blundy, J.D. 1994. Non-ideal interactions in calcic amphiboles and their bearing on amphibole-plagioclase thermometry. Contribution to Mineralogy and Petrology 116, 433-447.

Hollister, L.S., Grisson, G.C., Peters, E.K., Stowell, H.H., Sisson, V.B. 1987. Confirmation of the empirical calibration of aluminum in hornblende with pressure of solidification of calc-alkaline plutons. American Mineralogist 72, 231-239.

İlbeyli, N. 2008. Geochemical characteristics of the Şebinkarahisar granitoids in the Eastern Pontides, Northeast Turkey: petrogenesis and tectonic implications. International Geology Review 50, 563-582.

Jahn, B.M., Zhang, Z.Q. 1984. Archean granulite gneisses from eastern Hebei Province, China: rare earth geochemistry and tectonic implications. Contribution to Mineralogy and Petrology 85, 224-243.

Jiang, Y.H., Jiang, S.Y., Ling, H.F., Zhou, X.R., Rui, X.J., Yang, W.Z. 2002. Petrology and geochemistry of shoshonitic plutons from the western Kunlun orogenic belt, Xinjiang, northwestern China: implications for granitoid geneses. Lithos 63, 165-187.

Johnson, M.C., Rutherford, M.J. 1989. Experimental calibration of the aluminiun inhornblende geobarometer with application to Long Valley Caldera (California) volcanic rocks. Geology 17, 837-841.

Jung, S., Masberg, P., Mihm, D., Hoernes, S. 2009. Partial melting of diverse crustal sources constraints from Sr–Nd–O isotope compositions of quartz diorite–granodiorite–leucogranite associations (Kaoko Belt, Namibia). Lithos 111, 236-251.

Kandemir, R. 2004. Sedimentary characteristics and depositional conditions of Lower-Middle Jurassic Şenköy Formation in the around of Gümüşhane. Doktora Tezi, KTÜ, 274 s. Trabzon (unpublished).

Kandemir, R., Yılmaz, C. 2009. Lithostratigraphy, facies, and deposition environment of the lower Jurassic Ammonitico Rosso type sediments (ARTS) in the Gümüşhane area, NE Turkey: Implications for the opening of the northern branch of the Neo-Tethys

Ocean. Journal of Asian Earth Sciences 34, 586-598.

Karslı, O., Chen, B., Aydin, F., Şen, C. 2007. Geochemical and Sr-Nd-Pb isotopic compositions of the Eocene Dölek and Sarıçiçek Plutons, Eastern Turkey: implications for magma interaction in the genesis of high-K calc-alkaline granitoids in a post-collision extensional setting. Lithos 98, 67-96.

Karslı, O., Dokuz, A., Uysal, İ., Aydin, F., Bin, C., Kandemir, R., Wijbrans, R.J. 2010*a*. Relative contributions of crust and mantle to generation of Campanian high-K calc-alkaline I-type granitoids in a subdution setting, with special reference to the Harşit pluton, Eastern Turkey. Contributions to Mineralogy and Petrology 160, 467–487.

Karslı, O., Dokuz, A., Uysal, İ., Aydın, F., Kandemir, R., Wijbrans, R.J. 2010*b*. Generation of the early Cenozoic adakitic volcanism by partial melting of mafic lower crust, Eastern Turkey: implications for crustal thickening to delamination. Lithos 114, 109-120.

Karslı, O., Uysal, İ., Ketenci, M., Dokuz, A., Kandemir, R., Wijbrans, J. 2011. Adakite-like granitoid porphyries in the Eastern Turkey: potential parental melts and geodynamic implications. Lithos 127, 354-372.

Karslı, O., Caran, Ş., Dokuz, A., Çoban, H., Chen, B., Kandemir, R. 2012*a*. A-type granitoids from the Eastern Pontides, NE Turkey: Records for generation of hybrid A-type rocks in a subduction-related environment. Tectonophysics 530-531, 208-224.

Karslı, O., Dokuz, A., Uysal, İ., Ketenci, M., Chen, B., Kandemir, R. 2012*b*. Deciphering the shoshonitic monzonites with I-type characteristic, the Sisdağı pluton, NE Turkey: magmatic response to continental lithospheric thinning. Journal of Asian Earth Sciences 51, 45-62.

Karslı, O., Uysal, İ., Dilek, Y., Aydın, F., Kandemir, R. 2013. Geochemical modelling of early Eocene adakitic magmatism in the Eastern Pontides, NE Anatolia: continental crust or subducted oceanic slab origin?. International Geology Review 55, 16, 2083-2095.

Kaygusuz, A., Aydınçakır, E. 2009. Mineralogy, Whole-Rock and Sr-Nd Isotope Geochemistry of Mafic Microgranular Enclaves in Cretaceous Dağbaşı Granitoids, Eastern Pontides, NE Turkey: Evidence of Magma Mixing, Mingling, and Chemical Equilibration. Chemie der Erde/ Geochemistry 69, 247-277.

Kaygusuz, A., Aydınçakır, E. 2011. Petrogenesis of a Late Cretaceous composite pluton from the eastern Pontides: the Dağbaşı pluton, NE Turkey. Neues Jahrbuch Für Mineralogie 188, 3, 211-233.

Kaygusuz, A., Şen, C. 2011. Calc-alkaline I-type plutons in the eastern Pontides, NE Turkey: U-Pb zircon ages, geochemical and Sr-Nd isotopic compositions. Chemie der Erde Geochemistry 71, 59-75.

Kaygusuz, A., Öztürk,M. 2015. Geochronology, geochemistry, and petrogenesis of the Eocene Bayburt intrusions, Eastern Pontide, NE Turkey: implications for lithospheric mantle and lower crustal sources in the high-K calc-alkaline magmatism. Journal of Asian Earth Sciences 108, 97-116.

Kaygusuz, A., Siebel, W., Şen, C., Satır, M. 2008. Petrochemistry and petrology of I-type granitoids in an arc setting: the composite Torul pluton, Eastern Pontides, NE Turkey. International Journal of Earth Sciences 97, 739-764.

Kaygusuz, A., Chen, B., Aslan, Z., Siebel, W., Şen, C. 2009. U-Pb zircon SHRIMP ages, geochemical and Sr-Nd isotopic compositions of the Early Cretaceous I-type Sarıosman pluton, Eastern Pontides, NE Turkey. Turkish Journal of Earth Sciences 18, 549-581.

Kaygusuz, A., Siebel, W., İlbeyli, N., Arslan, M., Satır, M., Şen, C. 2010. Insight into magma genesis at convergent plate margins – a case study from the eastern Pontides (NE Turkey). Neues Jahrbuch Für Mineralogie 187, 3, 265-287.

Kaygusuz, A., Arslan, M., Siebel, W., Şen, C. 2011. Geochemical and Sr-Nd isotopic characteristics of post-collisional calc-alkaline volcanics in the eastern Pontides (NE Turkey). Turkish Journal of Earth Sciences 20, 137-159.

Kaygusuz, A., Arslan, M., Siebel, W., Sipahi, F., İlbeyli, N. 2012. Geochronological evidence and tectonic significance of Carboniferous magmatism in the southwest Trabzon area, eastern Pontides. Turkey, International Geology Review 54, 15, 1776-1800.

Kaygusuz, A,. Sipahi, F,. İlbeyli, N,. Arslan, M,. Chen, B,. Aydınçakır, E. 2013. Petrogenesis of the Late Cretaceous Turnagöl intrusion in the eastern Pontides: Implications for magma genesis in the arc setting. Geoscience Frontiers 4, 423-438.

Kaygusuz, A., Arslan, M., Wolfgang, S., Sipahi, F., İlbeyli, N., Temizel, İ. 2014. LA-ICP MS zircon dating, whole-rock and Sr-Nd-Pb-O isotope geochemistry of the Camiboğazı pluton, Eastern Pontides, NE Turkey: implications for lithospheric mantle and lower crustal sources in arc-related I-type magmatism. Lithos 192-195, 271-290.

Kaygusuz, A., Arslan, M., Sipahi, F., Temizel, İ. 2016. U–Pb zircon chronology and petrogenesis of Carboniferous plutons in the northern part of the Eastern Pontides, NE Turkey: Constraints for Paleozoic magmatism and geodynamic evolution. Gondwana Research 39, 327-346.

Ketin, İ. 1966. Anadolu'nun Tektonik Birlikleri, Maden Tetkik ve Arama Genel Müdürlüğü Dergisi 66, 20-34.

Köksal, S., Toksoy-Köksal, F., Göncüoğlu, M.C., Möller, A., Gerdes, A., Frei, D. 2013. Crustal source of the Late Cretaceous Satansarı monzonite stock (central Anatolia–Turkey) and its significance for the Alpine geodynamic evolution. Journal of Geodynamics 65, 82-93.

Lameyre, J., Bonin, B., 1991. Granites in the main plutonic series. In:Didier, J., Barbarin, B. (Eds.), Enclaves and GranitePetrology Developments in Petrology, vol. 13. Elsevier, Amsterdam.

Lan, T.G., Fan, H.R., Hu, F.F., Tomkins, A.G., Yang, K.F., Liu, Y.S. 2011. Multiple crust-mantle interactions for the destruction of the North China Craton: geochemical and Sr–Nd–Pb–Hf isotopic evidence from the Longbaoshan alkaline complex. Lithos 122, 87-106.

Lan, T.G., Fan, H.R., Santosh, M., Hu, F.F., Yang, K.F., Yang, Y.H., Liu, Y.S. 2012. Early Jurassic high-K calc-alkaline and shoshonitic rocks from the Tongshi intrusive complex, eastern North China Craton: implication for crust–mantle interaction and post-collisional magmatism. Lithos 140-141, 183-199.

Lan, T.G., Fan, H.R., Santosh, M., Hu, F.F., Yang, K.F., Yang, Y.H., Yang, Y.H., Liu, Y.S. 2013. Crust–mantle interaction beneath the Luxi Block, eastern North China Craton: evidence from coexisting mantle- and crust-derived enclaves in a quartz monzonite pluton. Lithos 177, 1-6.

Le Maitre, R.W., Streckeisen, A., Zanettin, B., Le Bas, M.J., Bonin, B., Bateman, P., Bellieni, G., Dudek, A., Efremova, S., Keller, J., Lamere, J., Sabine, P.A., Schmid, R., Sorensen, H., Woolley, A.R. 2002. Igneous Rocks: A Classification and Glossary of Terms, Recommendations of the International Union of Geological Sciences, Subcommission of the Systematics of Igneous Rocks. Cambridge University Press., 236p.

Le Roex, A.P. 1987. Source regions of mid-ocean ridge basalts; evidence for enrichment processes. In: Menzies, A.M., Hawkesworth, C.J. (Eds.), Mantle Metasomatism, Academic Press, London, 389-422.

Leake, E.B., Wooley, A.R., Arps, C.E.S., Birch, W.D., Gilbert, M.C., Grice, J.D., Hawthorne, F.C., Kato, A., Kisch, H.J., Krivovichev, V.G., Linthout, K., Laird, J., Mandarino, J., Maresch, W.V., Nickhel, E.H., Rock, N.M.S., Schumacher, J.C., Smith, D.C., Stephenson, N.C.N., Ungaretti, L., Whittaker, E.J.W., Youzhi, G. 1997. Nomenclature of amphiboles report of the subcommittee on amphiboles of the International Mineralogical Association Commission on New Minerals and Mineral Names. European Journal of Mineralogy 9, 623-651.

Li, X.H., Zhou, H.W., Liu, Y., Le, C.Y., Sun, M., Chen, Z.H. 2000. Shoshonitic intrusive suite in SE Guangxi: petrology and geochemistry. Chinese Sciences Bulletin 45, 653-659.

Li, X.H., Li, W.X., Li, Z.X., Lo, C.H., Wang, J., Ye, M.F., Yang, Y.H. 2009. Amalgamation between the Yangtze and Cathaysia Blocks in South China: constraints from SHRIMP U–Pb zircon ages, geochemistry and Nd–Hf isotopes of the Shuangxiwu volcanic rocks. Precambrian Research 174, 117-128.

Liu, H., Qiu, J.S., Luo, Q.H., Xu, X.S., Ling, W.L., Wang, D.Z. 2002. Petrogenesis of the Mesozoic potash-rich volcanic rocks in the Luzong basin, Anhui Province. geochemical constrains. Geochemica 31, 129-140.

Liu, L., Qiu, J.S., Li, Z. 2013. Origin of mafic microgranular enclaves (MMEs) and their host quartz monzonites from the Muchen pluton in Zhejiang Province, Southeast China: Implications for magma mixing and crust–mantle interaction. Lithos 160-161, 145-163.

Liu, L., Qiu, J.S., Zhao, J.L., Yang, Z.L. 2014. Geochronological, geochemical, and Sr–Nd–Hf isotopic characteristics of Cretaceous monzonitic plutons in western Zhejiang Province, Southeast China: new insights into the petrogenesis of intermediate rocks. Lithos 196-197, 242-260.

Liu, S., Hu, R.Z., Gao, S., Feng, C., Qi, Y.Q., Wang, T., Feng, G.Y., Coulson, I.M. 2008. U-Pb zircon age, geochemical and Sr–Nd–Pb–Hf isotopic constraints on age and origin of alkaline intrusions and associated mafic dikes from Sulu orogenic belt, Eastern China. Lithos 106, 365-379.

López-Moro, F.J., López-Plaza, M. 2004. Monzonitic series from the Variscan Tormes Dome (Central Iberian Zone): petrogenetic evolution from monzogabro to granite magmas. Lithos 72, 19-44.

Luhr, J.F., Carmichael, I.S.E., Varekamp, J.C. 1984. The 1982 eruptions of El Chicón Volcano, Chiapas, Mexico: Mineralogy and petrology of the anhydrite-bearing pumices. Journal of Vocanology and Geothermal Research 23, 69-108.

Maniar, P.D., Piccoli, P.M. 1989. Tectonic discrimination of granitoids. Geological Society of America Bulletin 101, 635-643.

Mao, J.R., Ye, H.M., Liu, K., Li, Z.L., Takahashi, Y., Zhao, X.L., Kee, W.S. 2013. The Indosinian collision–extension event between the South China Block and the Palaeo-Pacific plate: evidence from Indosinian alkaline granitic rocks in Dashuang, eastern Zhejiang, South China, Lithos 172-173, 81-97.

McKenzie, D., O'Nions, R.K. 1991. Partial melt distributions from inversion of rare earth element concentrations. Journal of Petrology 32, 1021-1091.

Middlemost, E.A.K. 1994. Naming materials in the magma/ igneous rock system. Earth Science Reviews 37, 215-224.

Miller, C.F., McDowell, S.M., Mapes, R.W. 2003. Hot and cold granites?: Implications of zircon saturation temperatures and preservation of inheritance. Geology 31, 529-532.

Miyashiro, A. 1978. Nature of alkalic volcanic rock series. Contributions to Mineralogy and Petrology 66, 91-104.

Morimoto, M., Fabries, J., Ferguson, A.K., Ginzburg, I.V., Ross, M., Seifert, F.A., Zussman, J., Aoki, K., Gottardi, G. 1988. Nomenclature of pyroxenes. Mineralogical Magazine 52, 535-550.

MTA, 2002. 1/500.000 ölçekli Türkiye Jeoloji Haritası, Samsun ve Trabzon Paftaları, Maden Tetkik ve Arama Genel Müdürlüğü, Ankara.

MTA, 2011. 1/100.000 ölçekli Türkiye Jeoloji Haritası, Giresun G39 Paftası, Maden Tetkik ve Arama Genel Müdürlüğü, Ankara.

Neves, S.P., Mariano, G. 1997. High-K calc-Alkalic plutons in Northeast Brazil: origin of the biotite diorite/ quartz monzonite to granite association and implications for the evolution of the Borborema Province. International Geological Review 39, 7, 621-638.

Okay, A.İ., Leven, E.J. 1996. Stratigraphy and paleontology of the upper Paleozoic sequences in the Pulur (Bayburt) region, Eastern Pontides. Turkish Journal of Earth Sciences 5, 145-155.

Okay, A.İ., Şahintürk, Ö. 1997. Geology of the Eastern Pontides. In: Robinson, A.G. (ed.), Regional and Petroleum Geology of the Black Sea and Surrounding Region. American Association of Petroleum Geologists Memoir 68, 291-311.

Okay, A.İ., Tüysüz, O. 1999. Tethyan sutures of northern Turkey", In: Durand, B., Jolivet, L., Hovarth, F., Séranne, M. (eds), The Mediterranean Basins: Tertiary Extension within the Alpine Orogen Tethyan Sutures of Northern Turkey. Geological Society London. Special Publications 156, 475-515.

Okay, A.İ., Sunal, G., Sherlock, S., Altıner, D., Tüysüz, O., Kylander-Clark, A.R.C, Aygül, M. 2013. Early Cretaceous sedimentation and orogeny on the active margin of Eurasia: Southern Central Pontides, Turkey. Tectonics 32, 1247-1271.

Patiño Douce, A.E. 1997. Generation of Metaluminous A-type Granites by Low-Pressure Melting of Calc-Alkaline Granitoids. Geology 25, 743-746.

Patiño Douce, A.E. 1999. What do Experiments Tell Us about the Relative Contributions of Crust and Mantle to the Origin of Granitic Magmas?. In: Understanding Granites: Intergrating New and Classical Techniques, (eds.): Castro, A., Fernandez, C., Vigneresse, J.L., Geological Society of London. Special Publication 168, 55-75.

Patiño Douce, A.E., Johnston, A.D. 1991. Phase Equilibria and Melt Productivity in the Pelitic System: Implications for the Origin of Peraluminous Granitoids and Aluminous Granulites. Contribution to Mineralogy and Petrology 107, 202-218.

Patiño Douce, A.E., Beard, J.S. 1996. Effects of P, f (O_2) and Mg/Fe Ratio on Dehydration Melting of Model Metagreywackes. Journal of Petrology 37, 999-1024.

Patiño Douce, A.E., McCarthy, T.C. 1998. Melting of crustal rocks during continental collision and subduction. In: When continents collide: Geodynamics and Geochemistry of Ultra-high Pressure Rocks, edited by Hacker, B. R., Liou, J. G., Kluwer Academic Publishers, Dordrecht, pp.27-55.

Pearce, J.A. 1983. The Role of Sub-Continental Lithosphere in Magma Genesis at Destructive Plate Margins. In: Continental Basalts and Mantle Xenoliths, (eds): Hawkesworth, C.J., Norry, M.J., Shiva Publishing, Cheshire, pp.230-249.

Pearce, J.A, Haris, N.B.W., Tindle, A.G. 1984. Trace element discrimination diagrams for the tectonic interpretation of granitic rocks. Journal of Petrology 25, 956-983.

Pearce, J.A., Bender, J.F., De Long, S.E., Kidd, W.S.F., Low, P.J., Güner, Y., Şaroğlu, F., Yılmaz, Y., Moorbath, S., Mitchell, J.J. 1990. Genesis of collision volcanism in eastern Anatolia Turkey. Journal of Volcanology and Geothermal Research 44, 189-229.

Pelin, S. 1977. Alucra (Giresun) Güneydoğu Yöresinin Petrol Olanakları Bakımından Jeolojik İncelenmesi. K.T.Ü. Yayınları, 87, 103s,Trabzon (unpublished)

Powell, R., 1984. Inversion of the assimilation and fractional crystallization (AFC) equations: characterization of contaminants from isotope and trace element relationships in volcanic suites. Journal of the Geological Society of London, 141, 447-452.

Putirka, K.D. 1999. Clinopyroxene+liquid equilibrium to 100 kbar and 2450 K. Contributions to Mineralogy and Petrology 135, 151-163.

Putirka, K.D. 2003. New igneous thermobarometers based on plagioclase + liquid equilibria. Eos. Trans. AGU, Fall Meeting. Suppl., Abstract 84, 46, F1583.

Putirka, K.D. 2005. Igneous thermometers and barometers based on plagioclase + liquid equilibria: Tests of some existing models and new calibrations. American Mineralogist 90, 336-346.

Putirka, K.D. 2008. Thermometers and barometers for volcanic systems. In Putirka, K.D., Tepley, F.E., Reviews in Mineralogy and Geochemistry 69, 61-120.

Putirka, K.D., Johnson, M., Kinzler, R., Walker, D. 1996. Thermobarometry of mafic igneous rocks based on clinopyroxene-liquid equilibria, 0-30 kbar. Contributions to Mineralogy and Petrology 123, 92-108.

Putirka, K.D., Ryerson, F.J., Mikaelian, H. 2003. New igneous thermobarometers for mafic and evolved lava compositions, based on clinopyroxene + liquid equilibria. American Mineralogist 88, 1542-1554.

Rapela, C.W., Pankhurst, R.J., 1996. Monzonite suites: the innermost Cordilleran plutonism of Patagonia. Transactions of the Royal Society of Edinburgh Earth Sciences 87, 193-203.

Rapp, R.P. 1995. Amphibole-out Phase Boundary in Partially Melted Metabasalt, its Control over Liquid Fraction and Composition, and Source Permeability. Journal of Geophysical Research 100, 15601-15610.

Rapp, R.P., Watson, E.B. 1995. Dehydration Melting of Metabasalt at 8–32 kbar: Implications for Continental Growth and Crust-Mantle Recycling. Journal of Petrology 36, 891-931.

Rapp, R.P., Watson, E.B. Miller, C.F. 1991. Partial Melting of Amphibolite Eclogite and the Origin of Archean Trondhjemites and Tonalites. Precambrian Research 51, 1-25.

Ridolfi F., Renzulli, A. 2012. Calcic amphiboles in calc-alkaline and alkaline magmas: thermobarometric and chemometric empirical equations valid up to 1130°C and 2.2 Gpa. Contributions to Mineralogy and Petrology 163, 877-895.

Ridolfi, F., Puerini, M., Renzulli, A., Menna, M., Toulkeridis, T. 2008. The magmatic feeding system of El Reventador volcano (Sub-Andean zone, Ecuador) constrained by texture, mineralogy and thermobarometry of the 2002 erupted products. Journal of Volcanology and Geothermal Research 176, 94-106.

Ridolfi, F., Renzulli, A., Puerini, M. 2010. Stability and chemical equilibrium of amphibole in calc-alkaline magmas: An overview, new thermobarometric formulations and application to subduction-related volcanos. Contributions to Mineralogy and Petrology 160, 45-66.

Roberts, M.P., Clemens, J.D. 1993. Origin of High-Potassium, Calcalkaline, I-Type Granitoids. Geology 21, 825-828.

Robinson, A.G., Banks, C.J., Rutherford, M.M., Hırst, J.P.P. 1995. Stratigraphic and structural development of the eastern Pontides, Turkey. Journal of the Geological Society, London 152, 861-872.

Rolland, Y., Perinçek, D., Kaymakcı, N., Sosson, M., Barrier, E., Avagyan, A. 2012. Evidence for ~80–75 Ma subduction jump during Anatolia-Tauride-Armenian block accretion and ~48 Ma Arabia-Eurasia collision in Lesser Caucasus-East Anatolia. Journal of Geodynamics 56-57, 76-85.

Rudnick, R.L., Gao, S. 2003. The composition of the continental crust. In: Rudnick, R.L. (Ed.), The Crust. In: Holland, H.D., Turekian, K.K. (Eds.), Treatise on Geochemistry 3. Elsevier-Pergammon, Oxford (64 pp).

Ryerson, F.J., Watson, E.B. 1987. Rutile saturation in magmas: implications for Ti-Nb-Ta depletion in island-arc basalts. Earth and Planetary Science Letters, 86, 225-239.

Schmidberger, S.S., Hegner, E. 1999. Geochemistry and isotope ststematics of calc-alkaline volcanic rocks from the Saar-Nahe basin (SW Germany)-implications for Late Variscan orogenic development. Contributions to Mineralogy and

Petrology 135, 373-385.

Schmidt, M.W. 1992. Amphibole composition in tonalite as a function of pressure: An experimental calibration of the Al-in-hornblende barometer. Contributions to Mineralogy and Petrology 110, 304-310.

Singh, J., Johannes, W. 1996. Dehydration Melting of Tonalites: Part II. Composition of Melts and Solids. Contributions to Mineralogy and Petrology 125, 26-44.

Skjerlie, K.P., Johnston, A.D.1996. Vapour-absent Melting from 10 to 20 kbar of Crustal Rocks that Contain Multiple Hydrous Phases: Implications for Anatexis in the Deep to very Deep Continental Crust and Active Continental Margins. Journal of Petrology 37, 661-691.

Smith, E.I., Sanchez, A., Walker, J.D., Wang, K.F. 1999. Geochemistry of mafic magmas in the hurricane volcanic field, Utah: implications for small- and large-scale chemical variability of the lithospheric mantle. Journal of Geology 107, 433-448.

Soesoo, A. 2000. Fractional crystallization of mantle-derived melts as a mechanism for some I-type granite petrogenesis: an example from Lachlan Fold Belt, Australia. Journal of Geological Society, London 157, 135-149.

Stevens, G., Clemens, J.D., Droop, G.T.R. 1997. Melt Production during Granulite Facies Anatexis: Experimental Data from ‘Primitive’ Metasedimentary Protoliths. Contributions to Mineralogy and Petrology 128, 352-370.

Streickeisen, A. 1976. To Each Plutonic Rock its Proper Name. Earth Science Review 12, 1–33.

Sun, S., McDonough, W.F. 1989. Chemical and isotopic systematics of oceanic basalt: Implications for mantle composition and processes. In: A.D. Saunders, M.J. Norry, (eds.), Magmatism in the Ocean Basins, Geological Society of London. Special Publication 42, 313-345.

Sun, C.G., Zhao, Z.D., Mo, X.X., Zhu, D.C., Dong, G.C., Zhou, S., Chen, H.H., Xie, L.W., Yang, Y.H., Sun, J.F., Yu, F. 2008. Enriched mantle source and petrogenesis of Sailipu ultrapotassic rocks in southwestern Tibet Plateau: constraints from zircon U–Pb geochronology and Hf isotopic compositions. Acta Petrologica Sinica 24, 249-264.

Şen, C. 2007. Jurassic volcanism in the Eastern Pontides: Is it rift related or subduction related?. Turkish Journal of Earth Sciences 16, 523-539.

Şen, C., Arslan, M., Van, A. 1998. Geochemical and petrological characteristics of the Eastern Pontide Eocene (?) alkaline volcanic province, NE Turkey. Turkish Journal of Earth Sciences 7, 231-239.

Şengör, A.M.C., Yılmaz Y. 1981. Tethyan Evolution of Turkey: A Plate Tectonic Approach. Tectonophysics 75, 181-241.

Taylor, S.R., McLennan, S.M. 1985. The Continental Crust, Its Composition and Evolution. Blackwell, Oxford, pp. 312.

Temizel, İ. 2014. Petrochemical evidence of magma mingling and mixing in the Tertiary monzogabbroic stocks around the Bafra (Samsun) area in Turkey: implications of coeval mafic and felsic magma interactions. Mineralogy and Petrology 108, 353-370.

Temizel, İ., Arslan, M. 2008. Petrology and geochemistry of Tertiary volcanic rocks from the İkizce (Ordu) area, NE Turkey: Implications for the evolution of the eastern Pontide paleo-magmatic arc. Journal of Asian Earth Sciences 31, 439-463.

Temizel, İ., Arslan, M. 2009. Mineral chemistry and petrochemistry of post-collisional Tertiary mafic to felsic cogenetic volcanics in the Ulubey (Ordu) area, eastern Pontides, NE Turkey. Turkish Journal of Earth Sciences 18, 29-53.

Temizel, İ., Arslan, M., Ruffet, G., Peucat, J.J. 2012*a*. Petrochemistry, geochronology and Sr-Nd isotopic systematics of the Tertiary collisional and post-collisional volcanic rocks from the Ulubey (Ordu) area, eastern Pontide, NE Turkey: implications for extension-related origin and mantle source characteristics. Lithos 128, 126-147.

Temizel, İ., Arslan, M., Abdioğlu, E., Yücel, C. 2012*b*. Bafra (Samsun) Yöresi Tersiyer Volkanitlerinin Petrografisi, Jeokimyası, Petrolojisi ve Jeodinamik Gelişimi. Karadeniz Teknik Üniversitesi BAP Projesi No: 1079, Trabzon.

Temizel, İ, Arslan, M., Abdioğlu, E., Yücel, C. 2014. Mineral chemistry and thermobarometry of the Eocene monzogabbroic stocks from the Bafra (Samsun) area in Turkey: implications for disequilibrium crystallization and emplacement condition. International Geology Review 56, 10, 1226-1245.

Temizel, İ., Arslan, M., Yücel, C., Abdioğlu, E., Ruffet, G. 2016. Geochronology and geochemistry of Eocene-aged volcanic rocks around the Bafra (Samsun, N Turkey) area: Constraints for the interaction of lithospheric mantle and crustal melts. Lithos 258-259, 92-114.

Thirlwall, M.F., Smith, T.E., Graham, A.M., Theodorou, N., Hollings, P., Davidson, J.P. Arculus, R.J. 1994. High field strength element anomalies in arc lavas; source or process?. Journal of Petrology 35, 3, 819-838.

Tischendorf, G., Gottesmann, B., Förster, H.J., Trumbull, R.B. 1997. On Li-bearing micas: Estimating Li from electron microprobe analyses and an improved diagram for graphical representation. Mineralogical Magazine 61, 809-834.

Topuz, G. 2002. Retrograde P–T path of anatectic migmatites from the Pulur Massif, Eastern Pontides, NE Turkey: petrological and microtextural constraints. 1st International Symposium of the Faculty of Mines (İTÜ) on Earth Sciences and Engineering Abstracts, Istanbul, Turkey, 110 p.

Topuz, G., Alther, R., Schwarz, W.H., Siebel, W., Satır, M., Dokuz, A. 2005. Post-Collisional Plutonism with Adakite-like Signatures: the Eocene Saraycık Granodiorite (Eastern Pontides, Turkey). Contributions to Mineralogy and Petrology 150, 441-455.

Topuz, G., Altherr, R., Schwarz, W.H., Dokuz, A., Meyer, H P. 2007. Variscan amphibolite-facies rocks from the Kurtoğlu metamorphic complex: Gümüşhane area, Eastern Pontides, Turkey. International Journal of Earth Sciences 96, 861-873.

Topuz, G., Altherr, R., Siebel, W., Schwarz, W.H., Zack, T., Hasözbek, A., Barth, M., Satır, M., Şen, C. 2010. Carboniferous High-Potassium I-Type Granitoid Magmatism in the Eastern Pontides: The Gümüşhane Pluton (NE Turkey). Lithos 116, 92-110.

Topuz, G., Okay, A.I., Altherr, R., Schwarz, W.H., Siebel, W. Zack, T., Satır, M., Şen, C. 2011. Post-collisional adakite-like magmatism in the Ağvanis Massif and implications for the evolution of the Eocene magmatism in the Eastern Pontides (NE Turkey). Lithos 125, 131-150.

Topuz, G., Çelik, Ö.F., Şengör, A.M.C., Altıntaş, İ. E., Zack, T., Rolland, Y., Barth, M. 2013. Jurassic Ophiolite Formation and emplacement as backstop to a subduction-accretion complex in Northeast Turkey, The Refahiye Ophiolite, and relation to the Balkan Ophiolites. American Journal of Science 313, 1054-1087.

Tulloch, A.J., Challis, G.A., 2000. Emplacement depths of Paleozoic–Mesozoic plutons from western New Zealand estimated by hornblende-Al geobarometry. New Zealand Journal of Geology and Geophysics 43, 555-567.

Turner, S., Arnaud, N., Liu, J., Rogers, N., Hawkesworth, C., Harris, N., Kelley, S., Van Calsteren, P., Deng, W. 1996. Post-collision shoshonitic volcanism on the Tibetan Plateau: implications for convective thinning of the lithosphere and the source of ocean island basalts. Journal of Petrology 37, 45–71.

Uchida, E., Endo, S., Makino, M. 2007. Relationship between solidification depth of granitic rocks and formation of hydrothermal ore deposits. Resource Geology 57, 47-56.

Ustaömer, T., Robertson, A.H.F. 1995. Palaeo-Tethyan tectonic evolution of the north Tethyan margin in the Central Pontides, N. Turkey. In: Geology of the Black Sea region (eds). Erler, A., Ercan, T., Bingöl, E., Örçen, S., MTA/JMO, 24-32.

Ustaömer, T., Robertson, A.H.F. 2010. Late Palaeozoic-Early Cenozoic tectonic development of the Eastern Pontides (Artvin area), Turkey: stages of closure of Tethys along the southern margin of Eurasia. In Stephonson, R.A., Kaymakcı, N., Sasson, M., Starostenko, V., Bergerat, F. (eds). Sedimentary Basin Tectonics from the Black Sea and Caucasus to the Arabian Platform. Geological Society, London. Special Publications 340, 281-327.

Ustaömer, T., Robertson, A.H.F., Ustaömer, P.A., Gerdes, A., Peytcheva, I. 2013. Constraints on Variscan and Cimmerian magmatism and metamorphism in the Pontides (Yusufeli–Artvin area), NE Turkey from U–Pb dating and granite geochemistry. in Robertson, A.H.F., Parlak, O., Ünlügenç, U.C. (eds). Geological Development of Anatolia and the Easternmost Mediterranean Region. Geological Society, London. Special Publications 372, 49-74.

Vielzeuf, D., Holloway, J.R. 1988. Experimental Determinations of the Fluid-absent Melting Reactions in the Pelitic System. Contributions to Mineralogy and Petrology 98, 257-276.

Wang, D., Ren, Q., Qui, J., Chen, K., Xu, Z., Zen, J. 1996. Characteristics of volcanic rocks in the shoshonite province, eastern China, and their metallogenesis. Acta Geologica Sinica 70, 23-34.

Wang, W., Liu, S.W., Bai, X., Li, Q. G., Yang, P.T., Zhao, Y. 2013. Geochemistry and zircon U–Pb–Hf isotopes of the late Paleoproterozoic Jianping diorite–monzonite–syenite suite of the North China Craton: implications for petrogenesis and geodynamic setting. Lithos 162-163, 175-194.

Watson, E.B., Harrison, T.M. 1983. Zircon saturation revisited: temperature and composition effects in a variety of crustal magma types. Earth and Planetary Science Letters 64, 295-304.

Weaver, B.L., Wood, D.A., Tarney, J., Joron, J. 1987. Geochemistry of Ocean Island Basalt from the South Atlantic: Ascension, Bouvet, St. Helena, Gough and Tristan da Cunda", In: Fitton, J.G. and Upton, B.G.J., Eds., Alkaline Igneous Rocks, The Geological Society London, Special Publication 30, 1, 253-267.

Wones, D.R. 1989. Significance of the assemblage titanite+magnetite+quartz in granitic rocks. American Mineralogist 74, 744-749.

Xu, Y.G., Huang, X.L., Ma, J.L., Wang, Y.B., Iizuka, Y., Xu, J.F., Wang, Q., Wu, X.Y. 2004. Crust–mantle interaction during the tectono-thermal reactivation of the North China Craton: constraints from SHRIMP zircon U–Pb chronology and geochemistry of Mesozoic plutons from western Shandong. Contribution to Mineralogy and Petrology 147, 750-767.

Yang, J.H., Wu, F.Y., Wilde, S.A., Xie, L.W., Yang, Y.H., Liu, X.M. 2007. Trace magma mixing in granite genesis: in-situ U–Pb dating and Hf-isotope analysis of zircons. Contribution to Mineralogy and Petrology 153, 177-190.

Yang, S.Y., Jiang, S.Y., Jiang, Y.H., Zhao, K.D., Fan, H.H. 2011. Geochemical, zircon U–Pb dating and Sr–Nd–Hf isotopic constraints on the age and petrogenesis of an Early Cretaceous volcanic-intrusive complex at Xiangshan, Southeast China. Mineralogy and Petrology 101, 21-48.

Yılmaz, Y. 1972. Petrology and structure of the Gümüşhane granite and surrounding rocks. NE Anatolia. PhD Thesis, Univ. of London.

Yılmaz, S., Boztuğ, D. 1996. Space and time relations of three plutonic phases in the Eastern Pontides, Turkey. International Geology Review 38, 10, 935-956.

Yılmaz, Y., Tüysüz, O., Yiğitbaş, E., Genç, Ş.C., Şengör, A.M.C. 1997. Geology and tectonics of the Pontides. in Robinson, A.G. (eds.), Regional and Petroleum Geology of the Black Sea and Surrounding Region. American Association of Petroleum Geologists Memoir 68, 183-226.

Yücel, C. 2013. Trabzon-Giresun arasındaki Tersiyer volkanitlerinin petrografisi, ^{40}Ar-^{39}Ar jeokronolojisi, petrokimyası, Sr-Nd-Pb izotop jeokimyası ve petrolojisi. Doktora Tezi, KTÜ Fen Bilimleri Enstitüsü, 406s, Trabzon (unpublished).

Yücel, C., Arslan, M., Temizel, İ., Abdioğlu, E., Ruffet, G. 2012. Trabzon- Giresun Arasındaki Tersiyer Alkalen Volkanitlerinin Tüm-Kayaç Petrokimyası ve ^{40}Ar-^{39}Ar Jeokronolojisi, KD Türkiye. 65. Türkiye Jeoloji Kurultayı Bildiri Özleri Kitabı 354-355.

Yücel, C., Arslan, M., Temizel, İ., Abdioğlu, E. 2014. Volcanic facies and mineral chemistry of Tertiary volcanics in the northern part of the Eastern Pontides, northeast Turkey: Implications for pre-eruptive crystallization conditions and magma chamber processes. Mineralogy and Petrology 108, 439-467.

Yücel, C., Arslan, M., Temizel, İ., Abdioğlu, E., Ruffet, G. 2017. Evolution of K-rich magmas derived from a net veined lithospheric mantle in an ongoing extensional setting: Geochronology and geochemistry of Eocene and Miocene volcanic rocks from Eastern Pontides (Turkey). Gondwana Research 45, 65-86.